ERDC/EL TR-08-32

US Army Corps
of Engineers®
Engineer Research and
Development Center

Environmental Quality and Installations Program

UXO Characterization: Comparing Cued Surveying to Standard Detection and Discrimination Approaches

Report 1 of 9
Summary Report

Stephen D. Billings

September 2008

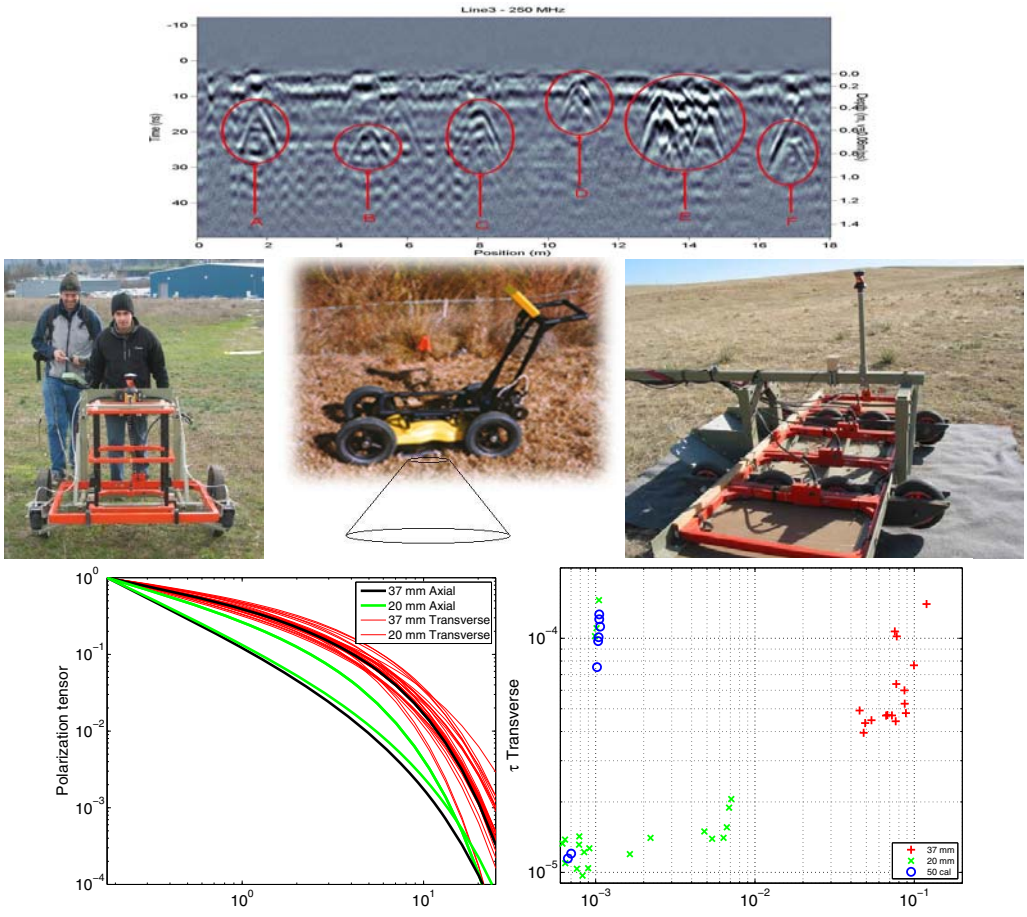

Environmental Laboratory

Environmental Quality and Installations Program

ERDC/EL TR-08-32
September 2008

UXO Characterization: Comparing Cued Surveying to Standard Detection and Discrimination Approaches

Report 1 of 9
Summary Report

Stephen D. Billings

Sky Research, Inc.
445 Dead Indian Memorial Rd.
Ashland, OR 97520-9706

Report 1 of 9

Prepared for Headquarters, U.S. Army Corps of Engineers
Washington, DC 20314-1000

Monitored by Environmental Laboratory
U.S. Army Engineer Research and Development Center
3909 Halls Ferry Road, Vicksburg, MS 39180-6199

Abstract: This report summarizes research conducted under W912HZ-04-C-0039 and highlights the most important results obtained. This project focused on determining the UXO discrimination potential of various sensor phenomenologies (ground penetrating radar, total-field magnetics, and time- and frequency-domain EMI), deployment modes, and processing strategies. Magnetometer and EMI sensors could be used for successful discrimination at each of the study sites. In each case, accurate position and orientation information and careful data collection, processing, and inversion were required to allow accurate feature vectors to be extracted over each detected anomaly. Once extracted, and with appropriate training data, effective discrimination strategies could be developed with the aid of statistical classification algorithms. Each site presented a different and novel discrimination challenge; multiple sensors, deployment modes, and interpretation strategies are required to tackle the diversity of UXO-contaminated sites in the United States and elsewhere.

Contents

Figures and Tables

Figures

Tables

Preface

This report was prepared as part of the Congressional Interest Environmental Quality and Installations Program, Unexploded Ordnance Focus Area, Contract No. W912HZ-04-C-0039, Purchase Request No. W81EWF-418-0425, titled, "UXO Characterization: Comparison of Cued Surveying to Standard Detection and Standard Discrimination Approaches." Research was conducted by Sky Research, Inc., for the Environmental Laboratory (EL), U.S. Army Engineer Research and Development Center (ERDC), Vicksburg, MS.

The following Sky Research personnel contributed to this report: Dr. Stephen D. Billings was the project PI and compiled this report by summarizing results from the other eight reports produced under this project; Terri Ayers was the copy editor for this report.

This project was performed under the general supervision of Dr. M. John Cullinane, Jr., Technical Director, Military Environmental Engineering and Sciences, EL; and John H. Ballard, Office of Technical Director and UXO Focus Area Manager, EL. Reviews were provided by Ballard and Dr. Dwain Butler, Alion Science and Technology Corporation. Dr. Beth Fleming was Director, EL.

COL Gary E. Johnston was Commander and Executive Director of ERDC. Dr. James R. Houston was Director.

Unit Conversion Factors

Multiply	By	To Obtain
acres	4,046.873	square meters
degrees (angle)	0.01745329	radians
inches	0.0254	meters

Acronyms

μs	microsecond(s)
ATS	Advanced Tracking Sensor
AUC	Area Under the Curve
cm	centimeters
COTS	Commercial Off The Shelf
DAS	Data Acquisition System
DoD	Department of Defense
DSB	Defense Science Board
EL	Environmental Laboratory
EM	Electromagnetic
EMI	Electromagnetic Induction
ERDC	Engineer Research and Development Center
ESTCP	Environmental Security Technology Certification Program
FAR	False Alarm Rate
FEM	Frequency Domain Electromagnetics
FLBGR	Former Lowry Bombing and Gunnery Range
FPGA	Field Programmable Gate Array
GPR	Ground Penetrating Radar
GPS	Global Positioning System
H/m	Henry per meter
IMU	Inertial Motion Unit
m	meter(s)
mm	millimeter(s)
ms	millisecond(s)
NSMC	Normalized Surface Magnetic Charge
OSU	Ohio State University

PNN	Probabilistic Neural Network
ROC	Receiver Operating Characteristic
RSS	Reduced Set of Sources
RTS	Robotic Total Station
SEA	Standardized Excitation Approach
SMC	Surface Magnetic Charge
SNR	Signal-to-Noise Ratio
SVM	Support Vector Machine
TEM	Time Domain Electromagnetics
TMC	Total Magnetic Charge
UXO	Unexploded Ordnance
USACE	U.S. Army Corps of Engineers

1 Introduction

The clearance of military facilities in the United States contaminated with unexploded ordnance (UXO) is one of the most significant environmental concerns facing the Department of Defense (DoD). A 2003 report by the Defense Science Board (DSB) on the topic estimated costs of remediation in the tens of billions of dollars. The DSB recognized that development of effective discrimination strategies to distinguish UXO from non-hazardous material is one essential technology area where the greatest cost saving to the Department of Defense can be achieved.

The objective of project W912HZ-04-C-0039 "UXO Characterization: Comparison of Cued Surveying to Standard Detection and Standard Discrimination Approaches," was to research, develop, optimize, and evaluate the efficiencies of different modes of UXO characterization and remediation as a function of the density of UXO and associated clutter. Survey modes investigated in the research include:

1. Standard detection survey: All selected anomalies are excavated;
2. Advanced discrimination survey: Data collected in proximity to each identified anomaly are inverted for physics-based parameters and statistical or analytical classifiers are used to rank anomalies, from which a portion of the higher ranked anomalies are excavated;
3. Cued-survey mode: Each selected anomaly is revisited with an interrogation platform, high-quality data are collected and analyzed, and a decision is made as to whether to excavate the item, or leave it in the ground.

Specific technical objectives of the research were to:

- Determine the feasibility and effectiveness of various interrogation approaches based on the cued-survey approach;
- Determine the feasibility and effectiveness of various interrogation sensors including magnetics, ground penetrating radar (GPR), and electromagnetic (EM) induction (EMI), and evaluate combinations of these sensors;
- Develop and evaluate the most promising interrogation platform designs;

- Develop optimal processing and inversion approaches for cued-interrogation platform datasets;
- Evaluate the data requirements to execute accurate target parameterization and assess the technical issues associated with meeting these requirements using detection and interrogation survey techniques;
- Determine which survey mode is most effective as a function of geological interference and UXO/clutter density;
- Investigate the feasibility and effectiveness of using detailed test stand measurements on UXO and clutter to assist in the design of interrogation algorithms used in the cued-search mode.

The main areas of research involved in these coordinated activities include:

- Sensor phenomenology including GPR, EMI , and magnetometry;
- Data collection systems; platforms, field survey systems, field interrogation systems;
- Parameter estimation techniques; inversion techniques (single, cooperative, joint), forward-model parameterizations, processing strategies; and
- Classification methods; thresholding, statistical models, information systems.

This report "UXO Characterization: Comparing Cued Surveying to Standard Detection and Discrimination Approaches: Report 1 of 9 – Summary Report" is one of a series of nine reports written as part of W912HZ-04-C-0039:

1. UXO Characterization: Comparing Cued Surveying to Standard Detection and Discrimination Approaches: Report 1 of 9 – Summary Report;
2. UXO Characterization: Comparing Cued Surveying to Standard Detection and Discrimination Approaches: Report 2 of 9 – Ground Penetrating Radar for Unexploded Ordnance Characterization; Fundamentals;
3. UXO Characterization: Comparing Cued Surveying to Standard Detection and Discrimination Approaches: Report 3 of 9 – Test Stand Magnetic and Electromagnetic Measurements of Unexploded Ordnance;

4. UXO Characterization: Comparing Cued Surveying to Standard Detection and Discrimination Approaches: Report 4 of 9 – UXO Characterization Using Magnetic, Electromagnetic and Ground Penetrating Radar Measurements at the Sky Research Test Plot;
5. UXO Characterization: Comparing Cued Surveying to Standard Detection and Discrimination Approaches: Report 5 of 9 – Optimized Data Collection Platforms and Deployment Modes for Unexploded Ordnance Characterization;
6. UXO Characterization: Comparing Cued Surveying to Standard Detection and Discrimination Approaches: Report 6 of 9 – Advanced Electromagnetic and Magnetic Methods for Discrimination of Unexploded Ordnance;
7. UXO Characterization: Comparing Cued Surveying to Standard Detection and Discrimination Approaches: Report 7 of 9 – Marine Corps Base Camp Lejeune: UXO Characterization Using Ground Penetrating Radar;
8. UXO Characterization: Comparing Cued Surveying to Standard Detection and Discrimination Approaches: Report 8 of 9 – Marine Corps Base Camp Lejeune: UXO Characterization Using Magnetic and Electromagnetic Data;
9. UXO Characterization: Comparing Cued Surveying to Standard Detection and Discrimination Approaches: Report 9 of 9 – Former Lowry Bombing and Gunnery Range: Comparison of UXO Characterization Performance Using Area and Cued-interrogation Survey Modes.

This report summarizes the work conducted under this research project and discusses implications for the future of UXO remediation.

2 Summary of Research Conducted

The research conducted here was focused on determining the UXO discrimination potential of various sensor phenomenologies, deployment modes, and processing strategies. Sensor phenomenologies explored included GPR, total-field magnetics, and time- and frequency-domain electromagnetic induction (TEM and FEM). Deployment modes developed included towed-array, cart-based, and man-portable in both discrimination and cued-interrogation modes. Processing strategies considered included static-dipole (for magnetics), polarization tensor, and physically complete approaches for electromagnetic induction.

The project focused on exploring the technical advantages and disadvantages of each method. While economic factors, like the time required to survey, were considered, a cost-benefit analysis of the different UXO remediation approaches was not conducted. This was intentional, as the applicability and relative costs of the different methods depend very strongly on various site-specific conditions such as geology, terrain, vegetation, number and variety of UXO and scrap items encountered, and on the costs of excavation of potential UXO, etc.

GPR explored the use of single and multi-polarization systems. The single polarization sensors included the Sensors and Software Noggin cart (for cued interrogation) and the Witten CART imaging system (for area surveys). Both of these systems were impulse (time-domain) systems with a center frequency of 400 MHz for the Witten system and either 250 or 1000 MHz for the Noggin system. The multi-polarization sensors comprised the Applied Research Associates Nemesis Advanced Ordnance Detection System (for area surveys) and the Ohio State University (OSU) research GPR (for cued interrogation). Both the Nemesis and OSU systems are stepped-frequency, continuous wave (SFCW) radar with operating ranges of 400 MHz to 4000 MHz (Nemesis) and 10 to 1000 MHz (OSU), respectively.

The GPR research was focused on determining the UXO detection and discrimination potential under various site conditions. These included the GPR “difficult” soils in the Ashland test plot and the GPR “friendly” soils at the Marine Corps Base Camp Lejeune. No new processing strategies were

developed in this project. Each dataset was processed by the project team using previously developed interpretation techniques. The GPR research is described in more detail in the next section and in Reports 2 and 7.

The test stand facility at the U.S. Army Corps of Engineers (USACE) Engineer Research and Development Center's (ERDC) Vicksburg site was used extensively in this project. High-quality magnetic, Geonics EM-61 (TEM), Geonics EM-63 (TEM) and Geophex GEM-3 (FEM) data were collected over 15 different UXO and 6 calibration cylinders at a number of different sensor-to-target distances and orientations (see Report 3 for a detailed description of the test stand data collection). The test stand surveys produced the highest quality data that one could conceivably collect with the respective sensors. These data served as a baseline to assess the discrimination ability of the various deployment modes and processing strategies. The data were also used extensively in the development of physically complete EMI forward-modeling methods, including the Standardized Excitations Approach (SEA) and the Surface Magnetic Charge (SMC) method. The theory for these methods was developed under SERDP project MM-1446 and expanded and refined as part of this project.

In addition to these new modeling methods, new strategies for the polarization tensor formulation commonly used as an interpretation tool for TEM and FEM data were also developed. A finger-printing approach was implemented, whereby the high-quality test stand data were used to define each object's polarization tensor. Using the data over an unknown item, the best-fitting position, depth, and orientation of each object in the library were determined. The anomaly source is assumed to be the item with the best match to the observed data. More details of the modeling methods are described in Section 4 of this report and in Report 6.

After characterization on the test stand, the UXO, calibration, and clutter objects were emplaced in a test plot at Sky Research's facility in Ashland, Oregon. This test plot allowed the project team to rapidly test different sensors and deployment modes to determine their suitability for deployment at one of the live sites. A number of different discrimination and cued-interrogation mode platforms were developed. These included a five-sensor EM-61 towed array, a suspension cart system for the EM-61 and EM-63, a template-based approach for the GEM-3 and another cart system for total-field magnetics. Integral to each deployment platform was a Leica TPS-1206 Robotic Total Station for sensor positioning, and a

Crossbow AHRS 400 Inertial Motion Unit for sensor orientation. Additional details on the sensor platforms developed are given in Chapter 5 and Report 5 of the series.

The first live site visited in this project was the Marine Corps Base Camp Lejeune in North Carolina. The primary focus of the Camp Lejeune mobilization was the assessment of the UXO detection and characterization abilities of the four GPR sensors mentioned earlier in this section. Results are summarized in Report 7. To support the GPR research, towed-array EM-61, cart-based EM-63, and man-portable magnetometer data were collected in discrimination mode over large sections of the site. Onsite ubiquitous aluminum adapters created a significant and unique discrimination challenge. Section 6.1 of this report and Report 8 describe the performance of the various magnetometer and EM methods.

The second live site visited was the Former Lowry Bombing and Gunnery Range (FLBGR) in Colorado. Two ranges were surveyed, partly to support this project and partly to support Environmental Security Technology Certification Program (ESTCP) Project MM-0504. The objectives of the Rocket Range surveys were the discrimination of a mixed range of projectiles with minimum diameter of 37 millimeters (mm) from shrapnel, junk, 20-mm projectiles, and small arms. The main ordnance item encountered was an MK-23 practice bomb. The 20-mm Range Fan survey presented a small-item discrimination scenario where the objective was to discriminate 37-mm projectiles from ubiquitous 20-mm projectiles and 50-caliber bullets. Towed-array EM-61, Geonics EM-63, and man-portable magnetometer data were collected in a discrimination mode. The results of those surveys are summarized in Section 6.2.2 with more details provided in the ESTCP discrimination report (Billings et al. 2007). The EM-63 and the GEM-3 were also deployed at the site in a cued-interrogation mode. These results are described in Sections 6.2.2 and 6.2.3 and in Report 9.

3 The Use of GPR for UXO Remediation

Radio waves are absorbed at different rates depending on the local survey environment, which results in finite, site-specific penetration depths. The Camp Lejeune site was chosen, in part, because the host soils were amenable to GPR signals. The location would serve as a "GPR friendly" site where the potential of GPR methods could be evaluated under relatively favorable conditions and contrasted with results from surveys at sites where the soils are less conducive to GPR surveying.

Two different modes of GPR surveying were employed. In discrimination mode surveying, data were collected over large areas by Witten Technologies CART imaging system and Applied Research Associates Nemesis Advanced Ordnance Detection. In the cued-interrogation surveying mode, targets previously identified in electromagnetic or magnetic data were flagged and resurveyed with a series of GPR profile passes over the marked area. The OSU multi-frequency, fully polarimetric system and a commercial off-the-shelf (COTS) GPR system were both deployed in this mode. For all systems, saturated ground conditions at Camp Lejeune at the time of the surveys resulted in significant attenuation of the GPR signal and degraded detection and characterization performance.

Array-based GPR systems were able to provide complete coverage over substantial areas. Witten Technologies CART imaging system covered over 3 acres during 5 days of surveying. The volume of data generated by full coverage GPR surveys is substantial. However, full coverage GPR may prove most valuable as a means to constrain EM or magnetometer interpretations. The Applied Research Associates Nemesis system also incorporates EMI sensors and correlating this with their GPSAR data produced encouraging results for the detection and discrimination of shallow UXO targets.

The COTS GPR system provided accurate depths to targets and confirmed the presence of multi-object scenarios when deployed in a cued-interrogation approach. While the inferred depths can be used to constrain inversions of EM data, detailed target information such as material properties, lengths, and aspect ratios are not attainable with a single polarization COTS GPR system. A cued-interrogation approach incorporating

OSU's fully polarimetric GPR system allowed for a more sophisticated classification of targets than the COTS cued-interrogation approach. An estimated linear factor could be calculated based on late time responses of the polarized data allowing targets to be deemed as UXO-like or non-UXO items.

In conclusion, even at a "favorable" site, UXO detection performance with a GPR system will vary throughout the year and will be dependant on the weather conditions at the site. The OSU, multi-frequency, multi-polarimetric system had the most promise and would be suitable for deployment as a confirmation sensor, particularly when the GPR interpretation is constrained by magnetic or electromagnetic data.

4 Advances in EM and Magnetic Interpretation Methods

Report 6 reviews the magnetic and EMI models and inversion strategies that are used to discriminate hazardous UXO from non-hazardous shrapnel and scrap metal. These two sensor technologies are the primary methods used for detection and discrimination of UXO. The most promising discrimination methods typically proceed by first recovering a set of parameters that specify a physics-based model of the object being interrogated. For EMI, a polarizability model is commonly used, which consists of two or three collocated orthogonal dipoles along with their orientation and some parameterization of the time-decay or frequency domain curve. For magnetics, the physics-based model is generally a static magnetic dipole. Once the parameters are recovered by inversion, a subset of the parameters is used as feature vectors to guide either a statistical or rule-based classifier.

Report 6 describes the dipole-based inversion and classification scheme. A number of variations to the scheme presented above are also considered, including:

1. Dipole-based template matching, where the object's identity is selected as the best fitting polarization model from a predefined library of objects;
2. Standardized Excitations Approach, where the dipole model is replaced with a more complete forward-modeling scheme. SEA is also a template-matching approach; and
3. Surface Magnetic Charge method, where the dipole model is replaced by a fictitious charge distribution on a circle or ellipse that encloses the UXO or clutter object. The total SMC is then used as a feature vector in a statistical or rule-based classification scheme.

4.1. Dipole-based methods

In the EMI method, a time-varying field illuminates a buried, conductive target. Currents induced in the target then produce a secondary field that is measured at the surface. EM data inversion involves using the secondary field generated by the target for recovery of the position, orientation, and parameters related to the target's material properties and shape. For UXO,

the inverse problem is simplified by assuming that the secondary field can be accurately approximated as a dipole.

In order to illuminate a buried target, TEM sensors generate a large primary field that is rapidly switched off. The currents induced in the buried target decay with time, generating a decaying secondary field that is measured at the surface. The time-varying secondary magnetic field $\mathbf{B}(t)$ at a location $\mathbf{r}$ from the dipole $\mathbf{m}(t)$ is

$$\mathbf{B}(t) = \frac{\mu_o}{4\pi r^3}\mathbf{m}(t) \times \left(3\hat{\mathbf{r}}\hat{\mathbf{r}} - \mathbf{I}\right) \tag{1}$$

where:

μ_o = $4\pi \times 10^{-7}$ Henry per meter (H/m) is the permittivity of free space

$\hat{\mathbf{r}} = \mathbf{r} / |\mathbf{r}|$ = unit-vector pointing from the dipole to the observation point

$r = |\mathbf{r}|$ = distance between the center of the object and the observation point.

$\mathbf{I}$ = 3×3 identity matrix.

Equation 1 assumes an ideal step-off field and can be modified to account for arbitrary transmitter waveforms. The dipole induced by the interaction of the primary field $\mathbf{B}_o$ and the buried target is given by

$$\mathbf{m}(t) = \frac{1}{\mu_o}\mathbf{M}(t) \cdot \mathbf{B}_o \tag{2}$$

where $\mathbf{M}(t)$ is the target's polarization tensor. The polarization tensor governs the decay characteristics of the buried target and is a function of the shape, size, and material properties of the target. The polarization tensor is written as:

$$\mathbf{M}(t) = \begin{bmatrix} L_1(t) & 0 & 0 \\ 0 & L_2(t) & 0 \\ 0 & 0 & L_3(t) \end{bmatrix} \tag{3}$$

where the convention $L_1(t_1) \geq L_2(t_1) \geq L_3(t_1)$ organizes polarization tensor parameters from largest to smallest.

As part of this project, a library- (or fingerprinting-) based technique was developed to identify UXO from time domain electromagnetic data. The high fidelity data acquired over a number of different ordnance items at the ERDC test stand (see Report 3) were inverted for polarization tensors. The polarization tensors are functions of the target only and, therefore, are used to characterize each member of the library. For each polarization tensor within the library, a template is generated. A template is defined as the data predicted by the polarization tensor that best fits the observed data. Generating this template requires solving a nonlinear inverse problem for the orientation and location of a target. Each of the data templates is then compared to the observed data. The template with the minimum error compared to the observed data is used to determine if the anomaly is generated by one of the targets. By not inverting for model parameters directly, tradeoffs between polarization tensor values and orientation and position that can occur are avoided. This method is not meant to replace parametric inversion, but rather provides an alternative discrimination strategy that may be better suited for certain discrimination scenarios.

A blind test of our prototype library/template matching code was performed using data collected over 10 items in the Sky Research test site (see Report 4). Data were collected in both dynamic and cued-interrogation modes. When performing the template matching algorithm on the dynamically collected data, 8 of 10 items were correctly identified (Table 1). When processing the statically collected data, 9 of 10 items were correctly identified.

Table 1. Results when applying the Fingerprinting/Template matching algorithm to dynamic and cued-interrogation style data.

Cell Label	Target Description	Predicted Target	
		Dynamic Data	Cued-interrogation
56d	40-mm M385	✓ 40-mm M385	✓ 40-mm M385
57b	BDU-28 submunition	✓ BDU-28 submunition	✓ BDU-28 submunition
60	81-mm M374 mortar	✓ 81-mm M374 mortar	✓ 81-mm M374 mortar
64c	M42 submunition	✓ M42 submunition	✓ M42 submunition
65a	MK 118 Rockeye	✓ MK 118 Rockeye	× 40-mm M385
67	2.75 in. rocket	✓ 2.75 in. rocket	✓ 2.75 in. rocket
68	2.75 in. rocket	✓ 2.75 in. rocket	✓ 2.75 in. rocket
71	M456 Heat Rd	× MN 76-mm	✓ M456 Heat Rd
72b	BLU-26 submunition	× M42 submunition	✓ BLU-26 submunition
73b	60-mm M493A	✓ 60-mm M493A	✓ 60-mm M493A

Figure 1 compares observed and predicted data when applying the library method to dynamically collected data measured over a 76-mm projectile. The data predicted using the 76-mm polarization parameters from the library produce the smallest misfit. Full details of the method are presented in Pasion et al. (2007).

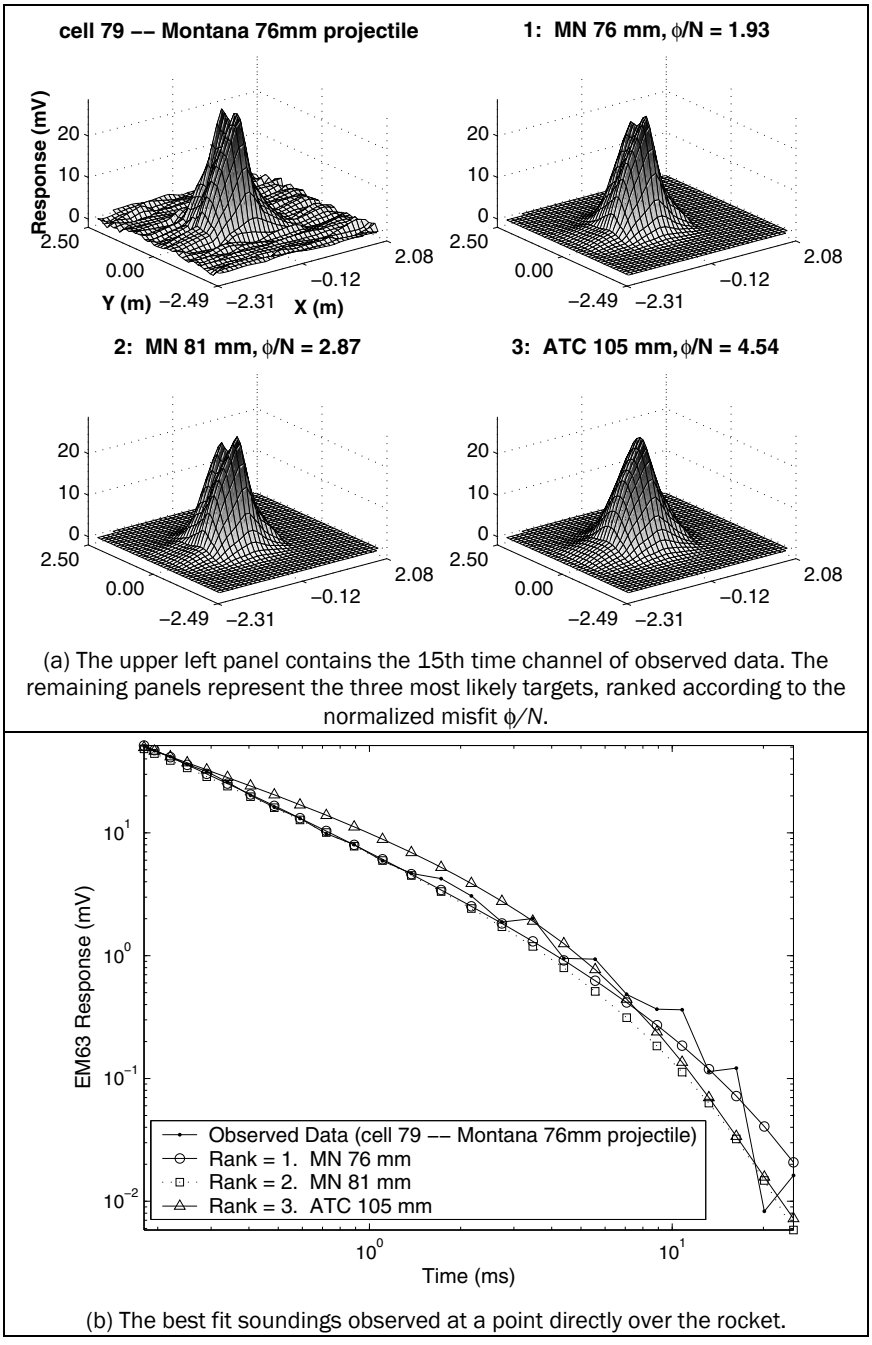

(a) The upper left panel contains the 15th time channel of observed data. The remaining panels represent the three most likely targets, ranked according to the normalized misfit ϕ/N.

(b) The best fit soundings observed at a point directly over the rocket.

Figure 1. Application of the library method to dynamically collected data measured over a 76-mm mortar. The objective is to determine which target in the library most likely fits the data.

4.2. Standardized excitations approach

The SEA is a numerical technique for computing the EMI response from a three-dimensional, electromagnetically heterogeneous object in both near and far fields. The objective of the SEA is to determine a set of characteristic sources, called the Reduced Set of Sources (RSS), associated with each UXO. These sources can then be used for fast modeling of the EMI response. The full EMI solution is obtained by the superposition of responses to the spheroidal excitation modes. A potential advantage of the SEA approach over that of the dipole model is that it is able to reproduce the signal from an arbitrary body at an arbitrary orientation and distance (both near and far-field).

Under the quasi-magnetostatic approximation, the magnetic field outside of an object is irrotational. For a primary field, the related primary potential ψ^{pr} on a fictitious spheroid $\xi = \xi_o$ surrounding the object can be expressed as:

$$\psi^{pr}(\eta, \xi, \varphi) = \frac{H_0 d}{2} \sum_{m=0}^{\infty} \sum_{n=m}^{\infty} \sum_{p=0}^{1} b_{pmn} P_n^m(\eta) P_n^m(\xi) T_{pm}(\varphi) \tag{4}$$

where (η, ξ, φ) are the standard prolate spheroidal coordinates, d is the inter-focal distance, P_n^m are associated Legendre functions of the first kind (Shubitidze et al. 2005b), and $T_{pm}(\varphi)$ is $\cos(m\varphi)$ for $p = 0$ and is $\sin(m\varphi)$ for $p = 1$. The coefficients b_{pmn} can be determined from the known primary field or potential. Equation 4 is a decomposition of a primary magnetic field $\left(-\Delta\psi^{pr}\right)$ into spheroidal modes.

After the primary magnetic field is decomposed into fundamental spheroidal modes, the secondary field due to an object can be written as a linear superposition of the object's response for each pmn excitation mode, i.e.,

$$\mathbf{H}_{sc}(\mathbf{r}) = \sum_{m=0}^{\infty} \sum_{n=m}^{\infty} \sum_{p=0}^{1} b_{pmn} \sum_{i=1}^{N_{red}} q_i^{pmn} \mathbf{G}(\mathbf{r}, \mathbf{r}_i') \tag{5}$$

where $\mathbf{r}$ is the position vector of an observation point outside of the object and q_i^{pmn} are the strength in the secondary field for the pmn mode at the i^{th} point $\mathbf{r}_i'$ distributed on a spheroidal surface and is called the RSS

(Shubitidze et al. 2005b), and $\mathbf{G}\left(\mathbf{r},\mathbf{r}_i'\right)$ is the Green's function for the magnetic field, given by

$$\mathbf{G}\left(\mathbf{r},\mathbf{r}_i'\right) = \frac{1}{4\pi\mu_0}\frac{\mathbf{r}-\mathbf{r}_i'}{\left|\mathbf{r}-\mathbf{r}_i'\right|^3} \tag{6}$$

It is observed from Equation 4 that the extrinsic characteristics in the secondary field are contained in the spheroidal modal expansion coefficients b_{pmn} determined by an excitation type, the location and orientation of the target, while the intrinsic characteristics of field response are separated in the RSS determined by the target's geometry and physics. This property of the RSS can make the SEA appealing to build libraries for the purpose of discrimination and classification regardless of what excitation is used.

There are two ways to determine q_i^{pmn}. One is to formulate the problem as an inverse problem and determine q_i^{pmn} for each mode, given the measured data. Obviously this process requires very detailed, low noise measurements, as well as techniques to reduce the problem of ill conditioning. The second method is a forward process to determine the amplitude q_i^{pmn} assuming that the geometry of an object and its physical properties are known. This is the procedure used for the work reported here. See Shubitidze et al. (2005b) for more details.

Full implementation of the SEA fingerprinting method would involve solving for the position and orientation that minimized the least-squares difference between the observed data and that predicted for each item in the library. The code to invert for location and orientation is being developed and is not mature enough to implement the nonlinear inversion approach. Therefore, a template-matching technique was developed to determine depth and orientation by searching a library of data pre-modeled at several depths and dip angles. Image registration was then used to find the location and azimuth angle of the target. The main objective of implementing this style of template matching is to determine if it is possible to identify targets using an RSS library without a priori information.

The first step of the algorithm is to generate a library of UXO responses. The generation of a library of UXO responses meant that all the forward

modeling using the RSS only needed to be performed once, thereby increasing the speed of the analysis. Target responses for nine ordnance items were calculated for target distances from the GEM3 sensor head varying, at 10-centimeter (cm) intervals, from 20 cm to 80 cm. At each depth the target was measured at dip angles from 0 deg (horizontal) to 90 deg (vertical), at 15-deg intervals. Data were modeled on 1-meter (m) square area and on a uniform grid with 10-cm spacing. UXO identification is achieved by cycling through the data templates in the library to determine the one that best matches the sensor data. However, the target location and azimuthal orientation are unknown. Determining the target location and azimuthal orientation is equivalent to determining the translation and rotation of the data templates. This operation represents a simple problem in image registration, since scaling the template does not need to be considered.

To demonstrate the above procedure, GEM3 data collected on the USACE ERDC Test Stand were used (see Report 3). A first example compares data from a horizontal 40-mm projectile located 30 cm from the GEM3 sensor head. Figure 2 compares the observed and modeled (for the best-fitting item) soundings directly over the center of the target. Figure 2(b) compares the misfit values for the different items in the RSS library. It is clear that C3 is the most likely target.

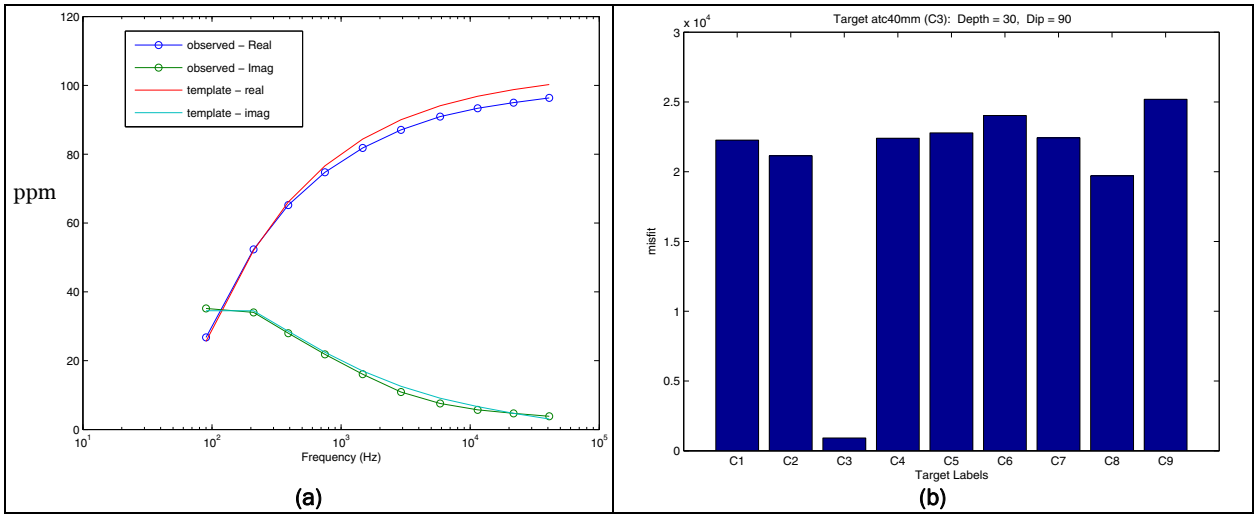

Figure 2. 40-mm projectile example: (a) data fit (with y-axis in parts-per-million, ppm); and (b) comparison of misfits.

4.3. The surface magnetic charge formulation

The SMC model (Shubitidze et al. 2005a) proposes a simple physical framework for describing the response of a metallic object to an inducing electromagnetic field. Like the SEA approach, it is applicable in both the near and far fields. However, in contrast to the SEA, the SMC is a parameter estimation technique and not a fingerprinting method. Thus statistical or rule-based classification can be applied to the estimated parameters in order to determine the UXO likelihood of an unknown, buried object.

The SMC model assumes a highly conducting, permeable, arbitrarily shaped, heterogeneous metallic target buried in soil with low conductivity. In a quasi-magneto static regime, displacement currents are negligible, conduction currents are weak outside the target, and the magnetic field is irrotational and can be written as the gradient of a scalar potential ψ:

$$\mathbf{H}^{\mathbf{sc}}\left(\mathbf{r},\xi\right) = -\nabla\Psi^{sc}\left(\mathbf{r},\xi\right) \tag{7}$$

where the variable ξ can represent either time t or frequency ω. If Gauss' Law is assumed for the magnetic field and if it is assumed that the field is generated by surface charges σ_m only, the magnetic field is given by:

$$\mathbf{H}^{\mathbf{sc}}\left(\mathbf{r},\xi\right) = \frac{1}{4\pi\mu_o}\int_S \sigma_m\left(\mathbf{r}',\xi\right)\frac{\left(\mathbf{r}-\mathbf{r}'\right)}{\left|\mathbf{r}-\mathbf{r}'\right|^3}dS' \tag{8}$$

where $\mathbf{r}$ is the observation point, $\mathbf{r}'$ is the source point, S is a closed surface surrounding the scatterer, and μ_o is the magnetic permeability of free space.

To numerically solve the SMC integral and define a charge distribution that characterizes a given type of ordnance, the surface S is split in sub-surfaces Δs_i assuming that the amplitude of σ_i, the surface magnetic charge at the center of Δs_i, is proportional to the normal component of the incident primary magnetic field at that point:

$$\sigma_i\left(\mathbf{r}',t\right) = q_i\left(\mathbf{r}',t\right)\left[\mathbf{H}^{\mathbf{pr}}\left(\mathbf{r}'\right)\cdot\hat{\mathbf{n}}\left(\mathbf{r}'\right)\right] = q_i\left(\mathbf{r}',t\right)\mathbf{H}_{\mathbf{n}}^{\mathbf{pr}}\left(\mathbf{r}'\right) \tag{9}$$

where q_i is the normalized magnetic charge surface density, assumed to be independent of the relative position of the sensor and target. Integration over the surface S defines the total Normalized Surface Magnetic Charge (NSMC) of an object at a given time channel (or frequency) as:

$$Q(t) = \sum_{i=1}^{N} q_i(\mathbf{r}', t)\Delta S_i \tag{10}$$

Pasion et al. (2006) applied the SMC model to the UXO problem, and found that the SMC provided accurate data prediction and demonstrated potential for discrimination of a large collection of standard UXO. Figure 3 shows the total NSMC calculated using Geonics EM-63 data collected on the test stand over a variety of objects including UXO, pieces of scrap, and several cylindrical calibration objects. The total magnetic charge (TMC) for each item is unique enough to make discrimination between object types feasible (at least on data with dense coverage, high signal-to-noise ratio (SNR), and accurate positioning).

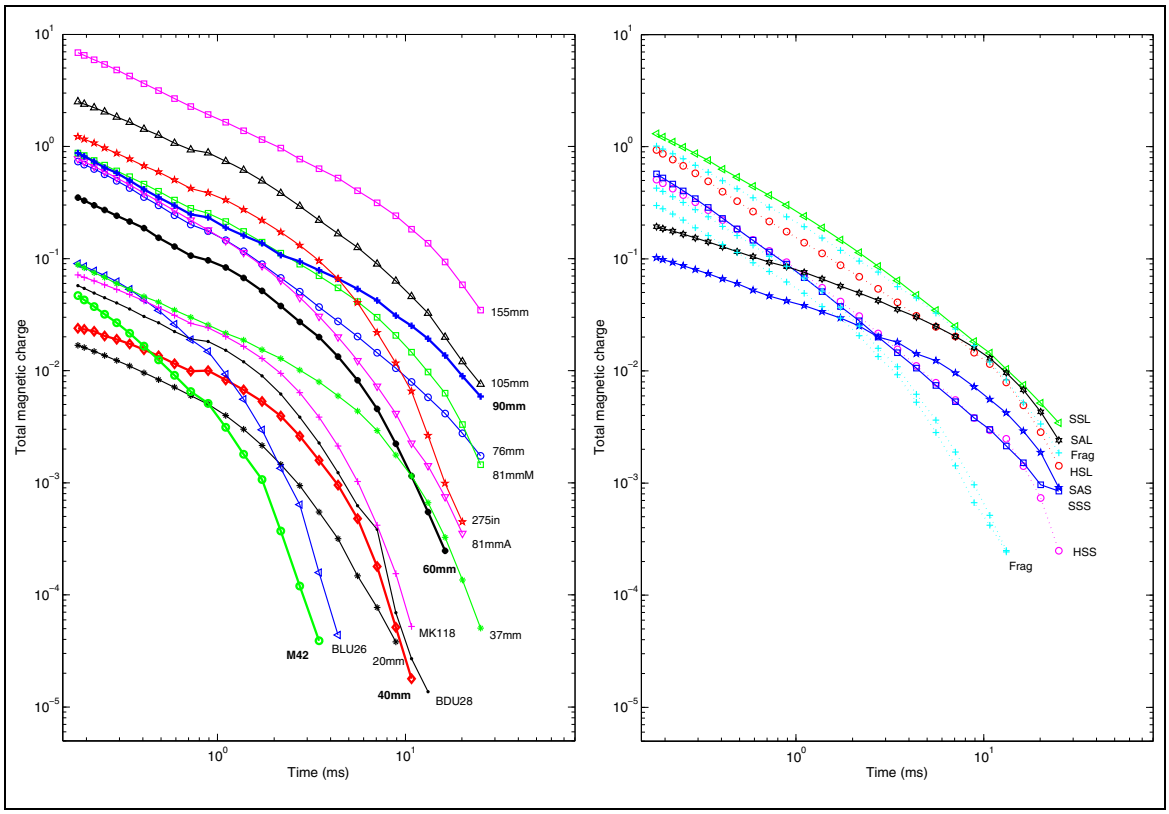

Figure 3. Total magnetic charge recovered from EM-63 data collected over a range of ordnance (left) and cylinders (right). Each curve is labeled with the identity of the item used. SSL = solid-steel-long; SAL = solid-aluminum-long; HSL = hollow-steel-long; SSS = solid-steel-short; SAS: = solid-aluminum-short; HSS = hollow-steel-short.

4.4. Conclusions

This project explored a number of different forward models and inversion procedures that are used to aid UXO discrimination from magnetic and time- and frequency-domain electromagnetic data. The simplest and most widely used magnetic and EMI models are based on dipoles: a static dipole in the magnetic case, and a polarization tensor formulation for EMI. The dipole model parameters can act as feature-vector inputs to a statistical or rule-based classification scheme to determine their UXO likelihood. Alternatively, using high-quality test stand data, a library of polarization tensor models can be created and a template or fingerprint matching scheme can be implemented to determine the identity of each buried object. Both of these dipole-based methods are well developed and were used extensively in this project (e.g., for the live-site deployments to FLBGR and Camp Lejeune described later). In addition, the methods are undergoing test and evaluation at a number of live sites through the ESTCP program.

The advantage of the SEA and SMC methods is that, unlike the dipole model, they are able to reproduce the response of an object in both the near and far-fields. However, the methods are not yet as mature as the dipole model, and the work described herein must be considered preliminary. Neither method can currently be used for discrimination of live-site data. In addition, neither method has demonstrated a clear, practical advantage over the dipole-based methods at this time.

5 Improvements to Sensor Systems

A significant component of the work conducted under this contract involved the modification and development of discrimination and cued-interrogation platforms and procedures. For primary positioning (Figure 4), each of the developed systems used the Leica TPS-1206 Robotic Total Station (RTS) in place of a Global Positioning System (GPS). A Crossbow AHRS 400 Inertial Measurement Unit (IMU) was used to provide sensor orientation information and to further refine the RTS positions (Figure 4). Report 5 describes each of the modifications and compares the performance of the modified system against a baseline system.

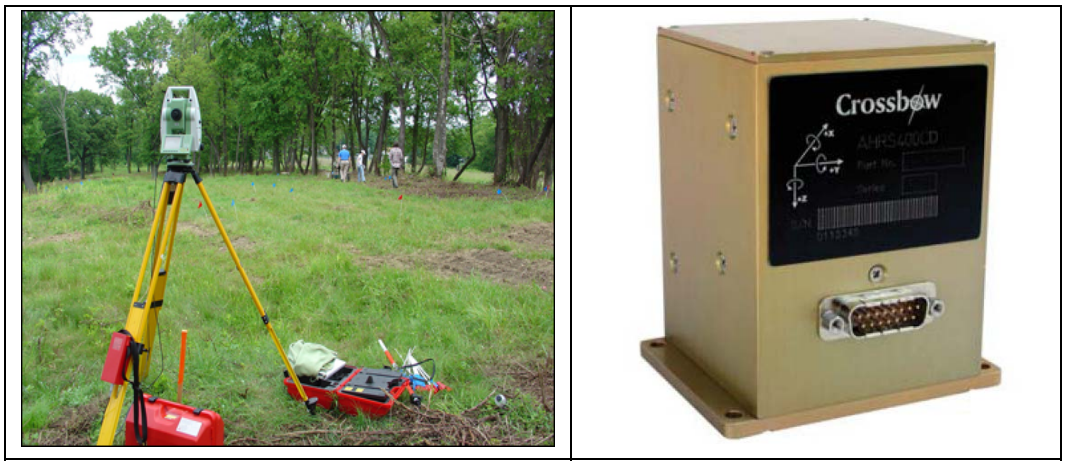

Figure 4. Sky Research utilizes the Leica RTS TPS1206 laser positioning system (left) and the Crossbow AHRS 400 Inertial Motion Unit for sensor orientation (right).

5.1. Discrimination mode platforms

The following discrimination mode platforms were modified or developed as part of this research project:

1. Sky Research's existing three-element EM-61 towed array was upgraded to a five-element towed array with a Crossbow IMU for sensor orientation and refinement of array positioning (Figure 5a). A second prism on the far corner of the array (the longest lever arm in the system) tested the positional accuracy of the system. Without using the IMU, 90 percent of positions were measured within 23 cm of the actual location with a maximum error of 45 cm. The inclusion of the IMU significantly improved the positional accuracy of the system as 90 percent of IMU-aided locations were

within 8 cm of the measured location with a maximum error of 30 cm (see Report 5).

(a) Geonics EM-61 towed array

(b) Geonics EM-61

(c) Geonics EM-63

(d) Total field magnetometer

Figure 5. Discrimination mode platforms developed under this project.

2. Modifications to the Geonics EM-61 cart-based sensor systems to incorporate an RTS for positioning and a crossbow IMU for orientation, as well as a suspension system (Figure 5b). The Ashland test plot was used to compare the performance of the new system against a production standard EM-61 positioned with GPS. Three-dipole instantaneous polarization fits to the new system had more accurate locations and depths (compared to

ground-truth) than the production standard EM-61. In addition, polarization parameters for each class of ordnance were more tightly clustered indicating that the new system has superior discrimination ability (see Report 5).

3. Geonics EM-63 suspension cart with RTS positioning and Crossbow IMU for orientation (Figure 5c). The Ashland test plot was used to compare the performance of the new system against an EM-63 positioned with GPS alone. Three-dipole Pasion-Oldenburg fits to the new system had more accurate locations and depths than the EM-63 with GPS. In addition, polarization parameters for each class of ordnance were more tightly clustered indicating that the new system has superior discrimination ability (see Report 5).
4. Geometrics G823 magnetometer man-portable quad-sensor array and cart, both with RTS positioning and Crossbow IMU for orientation (Figure 5d). Dipole moment depths and locations predicted from the cart data were more accurate than those predicted from a production level man-portable magnetometer array (see Report 5).

5.2. Cued-interrogation mode platforms

In addition to the modifications described above to discrimination mode systems, the following cued-interrogation platforms/procedures were developed:

1. EM-63 cued-interrogation procedure based on the RTS/IMU/suspension cart and a “magic carpet” comprising a 2.5-m by 2.5-m tarpaulin with lanes pre-marked at 25-cm spacing (Figure 6a). Three-dipole Pasion-Oldenburg fits to EM-63 data collected from the Ashland test plot were used to compare the parameters recovered from discrimination and cued-interrogation data with those recovered from “near-perfect” EM-63 data collected on the test stand. The cued interrogation and test stand parameters were in close agreement indicating that the cued-interrogation strategy provides superior discrimination performance.
2. GEM-3 cued-interrogation procedure based on 40-cm sensor head and a 1-m by 1-m plywood template (Figure 6b). Performance results obtained at the FLBGR live site demonstrated the excellent discrimination performance of this system.

(a) Geonics EM-63

(b) Geophex GEM-3

Figure 6. Cued-interrogation mode platforms developed under this project: (a) EM-63 and (b) GEM-3.

5.3. Final comments on deployed platforms

Each of the sensor platforms utilized the Leica TPS 1206 RTS for sensor positioning and used a Windows XP-based Data Acquisition System (DAS) for time stamping and storage of the asynchronous data streams. There are two limitations with these system components:

1. Inaccurate time stamping of sensor measurements by the Windows-based DAS. At best, the Windows Operating System is able to time stamp events appearing on a serial port with accuracies between 10 and 20 milliseconds. Recognizing this limitation, a hardware-based DAS was developed that uses a Field Programmable Gate Array (FPGA) and a real-time Linux Operating System. This system can simultaneously time stamp multiple events with an accuracy of 10 microseconds. Unfortunately, this system was not ready in time for this project but has subsequently been used for collection of EM-63 data at Camp Sibert, AL as part of an ESTCP-sponsored demonstration.
2. As described in Report 5 of this series, the Leica TPS 1206 outputs its positions at variable latencies, which can cause errors in time-stamping as large as 0.1 second or more. This is a firm-ware limitation of the Leica system and there are no immediate plans to fix it. Fortunately, Trimble has introduced a new RTS, the Trimble Advanced Tracking Sensor (ATS),

which uses an active prism, has very small latency, and has very little jitter in the latency time. The ATS system should significantly improve the time stamp (and hence) positional accuracy of the collected sensor data.

6 Live Sites Comparison of Survey Modes

Two live sites were visited as part of this research project:

1. Marine Corps Base Camp Lejeune in North Carolina: Magnetometer, EM-61, and EM-63 data were collected there in a discrimination mode. The discrimination challenge at the site was to identify large ferrous UXO and non-ferrous 40-mm grenades without excessive excavations of false alarms, particularly non-ferrous adapters that were common on the site.
2. Former Lowry Bombing and Gunnery Range in Colorado: Magnetometer, EM-61, and EM-63 data were collected in a discrimination mode and EM-63 and GEM-3 data in a cued-interrogation mode. Two ranges were surveyed; each had a different discrimination challenge. At the Rocket Range, the objective was to discriminate a wide variety of UXO from nonhazardous shrapnel and range debris. At the 20-mm Range Fan, the objective was to distinguish hazardous 37-mm projectiles from less hazardous 20-mm and 50-caliber bullets.

6.1. Marine Corps Base Camp Lejeune

A total of 837 anomalies were excavated at the G-6 Range at Camp Lejeune, including 30 emplaced ordnance, a 120-mm rocket, and a large number of 40-mm smoke or practice grenades. Pervasive on the site were non-ferrous adapters, which comprised almost 40 percent of the items excavated. The discrimination challenge at the site was to identify larger ferrous UXO and the smaller 40-mm grenades while preventing excessive excavations of adapters.

The insensitivity of magnetometry to non-ferrous metals made it an ideal technique for rejecting false alarms due to the ubiquitous adapters present on the site. However, this same argument precluded using the technique for detection of the 40-mm grenades. For the emplaced UXO items, prioritizing digging order based on the magnetic remanence metric was very effective on all but three of the emplaced UXO (which exhibited large remanent magnetization). A more conservative and safer method was to dig according to the size of the moment and would have resulted in the excavation of just over half of the detected items.

For the EM-61 towed array, the spread of secondary to tertiary polarizations, or the ratio of primary to secondary polarization of the three-dipole models did not provide any useful discrimination information. After turning the three-dipole models into equivalent two-dipole models, the relative size of primary and secondary polarizations allowed many adapters to be rejected. The relative decay rate of the primary or secondary polarizations was effective in distinguishing many of the remaining adapters from the UXO (Figure 7). The standard deviation in a 0.5-m radius of the corresponding magnetic data was also highly discriminatory against the adapters (Figure 7).

For the EM-63 cart data, the decay of the secondary polarization of the adapters was significantly different than that of any of the UXO (Figure 7). Consequently, the Pasion-Oldenburg k_1, k_2, β_2 and γ_2 feature vectors were very effective in discriminating UXO from adapters, and the 40-mm grenades from the adapters (Figure 8). The longer measurement time of the EM-63 resulted in superior discrimination performance to the EM-61 and obviated the need for supplemental magnetic data. For the UXO/adapter discrimination problem, the EM-61/magnetometer combination performed comparably to the EM-63 alone. When the 40-mm grenades were included as potential UXO, the EM-63 significantly outperformed the EM-61/magnetometer combination (Figure 8 and Table 2).

More details of the Camp Lejeune results can be found in Report 8 of this series.

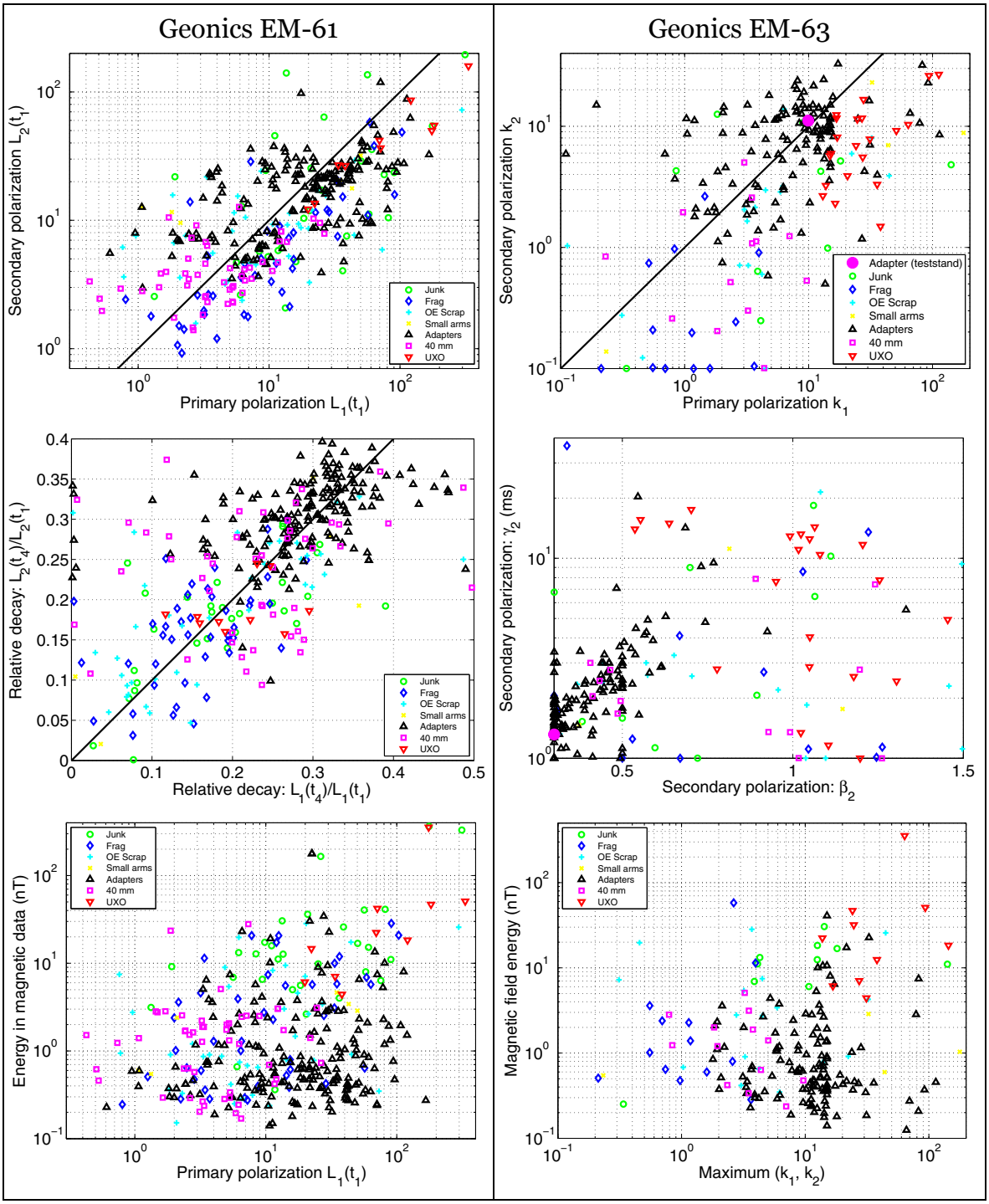

Figure 7. Feature vectors extracted from EM-61 (left row) and EM-63 data (right row).

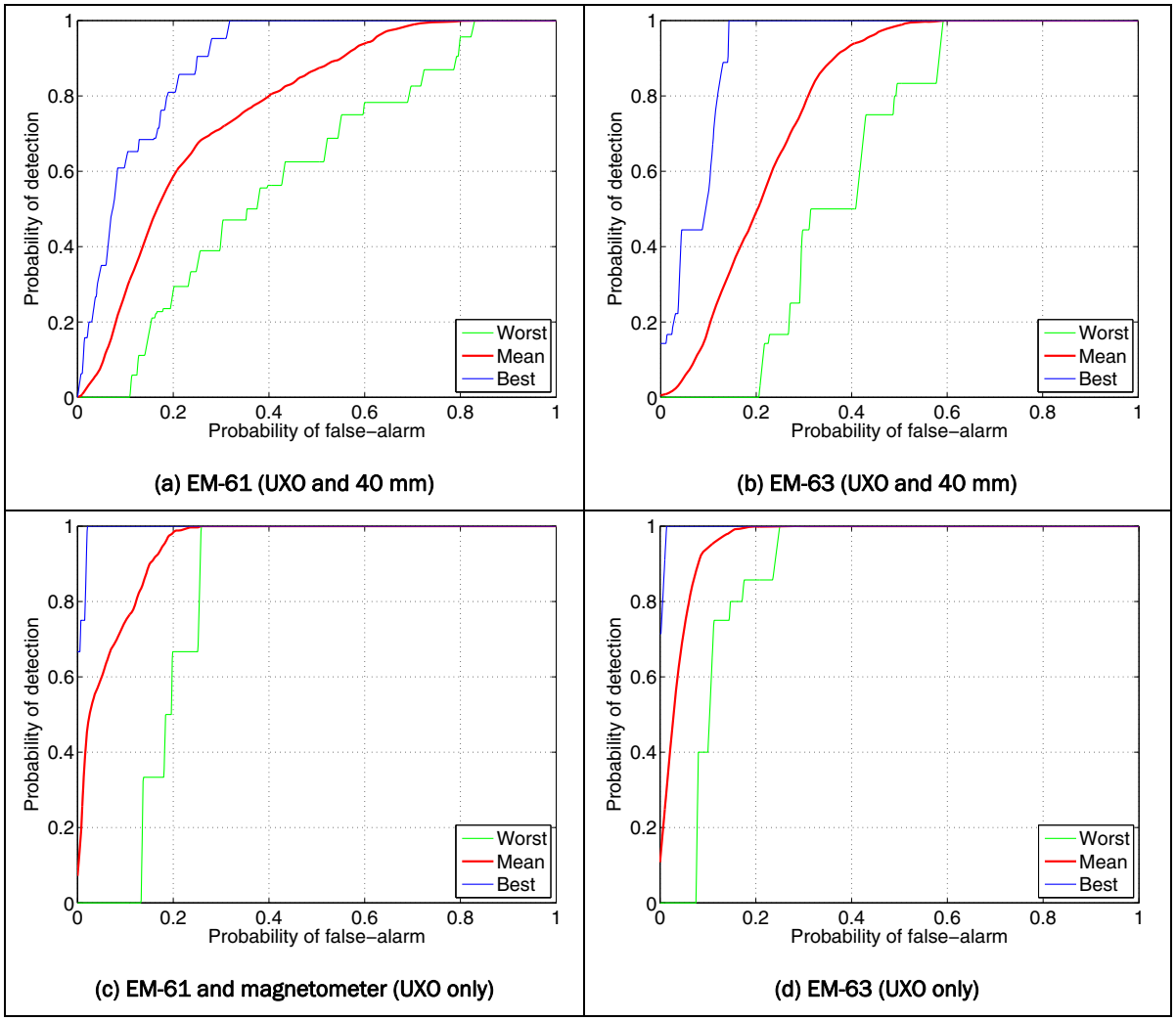

Figure 8. Comparison of best, worst, and mean receiver operating characteristic (ROC) curves through bootstrapping of various discrimination methods applied to the EM-61 array (left column) and EM-63 (right column) data. The objective for the top row was to distinguish UXO and 40 mm from adapter, while for the bottom row the objective was UXO from adapters: (a) EM-61 PNN trained on $L_2(t_1)$ and $L_2(t_4)/L_2(t_1)$; (b) and (d) EM-63 PNN trained on k_1, β_2, γ_2; (c) EM-61 PNN trained on $L_2(t_1)$ and magnetic-field energy.

Table 2. Comparison of statistical classifiers applied to the EM-61 towed-array data

Probablistic Neural Network (PNN) Trained Using:	Finding 40-mm Grenades		Finding UXO	
	Area Under the Curve (AUC)	False Alarm Rate (FAR)	AUC	FAR
EM-61 using $L_2(t_1)$, $L_2(t_4)/ L_2(t_1)$	0.85	0.66	0.91	0.20
EM-61 $L_2(t_1)$, magnetics	0.86	0.86	0.94	0.13
EM-63 using k_1, β_2, γ_2	0.79	0.4	0.94	0.13
EM-63 using k_1, magnetics	0.71	0.88	0.89	0.25

6.2. Former Lowry Bombing and Gunnery Range

The work at FLBGR was conducted jointly with ESTCP Project MM-0504 and occurred with significant logistical support from the USACE-Omaha District. Two ranges were surveyed with the modified discrimination mode systems described in Report 5: the Geonics EM-61 towed-array; the Geonics EM-63; and a total-field magnetometer. The objectives of the Rocket Range surveys were the discrimination of a mixed range of projectiles with minimum diameter of 37 mm from shrapnel, junk, 20-mm projectiles, and small-arms/munitions. The main ordnance item encountered was an MK-23 practice bomb. The 20-mm Range Fan survey presented a small-item discrimination scenario where the objective was to discriminate 37-mm projectiles from ubiquitous 20-mm projectiles and 50-caliber bullets. Cued-interrogation data were collected with the Geonics EM-63 on both sites and with the Geophex GEM-3 sensors on the 20-mm Range Fan.

6.2.1. Analysis of discrimination mode data

Two phases of digging and training were performed at the 20-mm Range Fan, and three phases at the Rocket Range. At the Rocket Range, 29 MK-23 practice bombs were recovered, with only one other UXO encountered (a 2.5-in. rocket warhead). At the 20-mm Range Fan, 38 37-mm projectiles (most of them emplaced) were recovered, as were a large number of 20-mm projectiles and 50-caliber bullets. For both sites, and for both instruments (EM-61 and EM-63), a Support Vector Machine (SVM) classifier outperformed a ranking based on amplitude alone (Figure 9). The SVM classifier used two feature vectors: one related to size and the other to goodness of fit. In each case, the last detected UXO was ranked quite high by the SVM classifier and digging to that point would have resulted in a 60-90 percent reduction in the number of false alarms. This operating point is of course unknown prior to digging. Using a stop-digging criteria mid-way between UXO and clutter class support planes was found to be too aggressive and more excavations were typically required for full recovery of detected UXO. Both the amplitude and SVM methods performed quite poorly on two deep (40-cm) emplaced 37-mm projectiles at the 20-mm Range Fan, exposing a potential weakness of the goodness of fit metric. Retrospective analysis revealed that thresholding on the size of the polarization tensor alone would have yielded good discrimination performance.

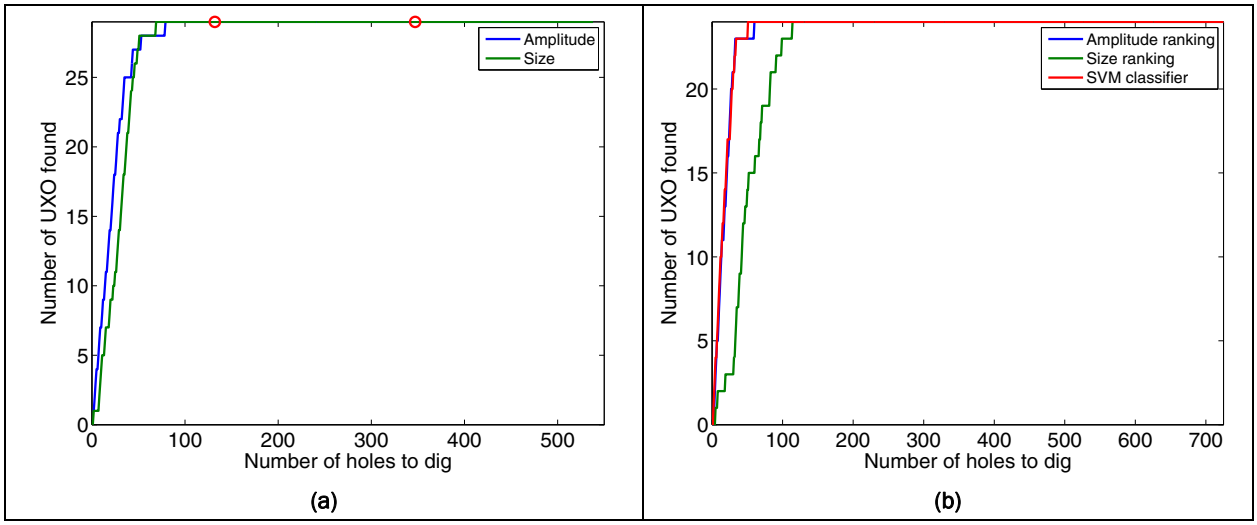

Figure 9. Receiver operating characteristic curves for the (a) EM-61 and (b) EM-63 discrimination methods at the Rocket Range.

At the 20-mm Range Fan, 50-caliber bullets caused more false alarms than 20-mm projectiles, even though they are significantly smaller. Retrospective analysis revealed that this was caused by a lower SNR[1] on the 50-caliber bullets. There was insufficient SNR to constrain the depth of the item and inversion solutions tended to be pushed deep due to either flat-objective functions or the presence of multiple locally optimal solutions. Consequently, size estimates of 50-caliber bullets obtained from the amplitude of the polarization tensor varied across four orders of magnitude and tended to be overestimated. For the larger 20- and 37-mm projectiles, size estimates varied by approximately two orders of magnitude, but there was less overlap between the two classes. Relatively poor depth performance on shallow, high SNR MK-23 practice bombs at the Rocket Range indicates that positional errors (and potentially unmodeled dipole components) also cause uncertainty in the object depth (and hence in the object size). This indicates that depth and size are poorly constrained when estimated from single component sensor data obtained with currently available positional accuracy. However, size estimates may still provide useful information to prioritize digging order.

During the demonstration, feature vectors derived from the time-decay properties of the polarization tensor were not used to aid discrimination performance of either instrument. The noise-floor decays as $1/t^{0.5}$ while signal falls off more rapidly. This means that the accuracy of time-decay

[1] Positioning error and sparse data coverage also likely contributed to the inability to constrain size.

parameters extracted from low SNR anomalies are generally limited. However, retrospective analysis revealed that, for both instruments, time-decay properties of the principal polarization tensor could have been used to distinguish MK-23 practice bombs from other items on the Rocket Range (Figures 10 and 11). On the 20-mm Range Fan, the time range of the EM-63 is long enough to distinguish the slower decay rate of the 37-mm projectiles from 20-mm projectiles (Figures 12 and 13). In contrast, the EM-61 did not sample late enough in time to aid discrimination (Figure 13).

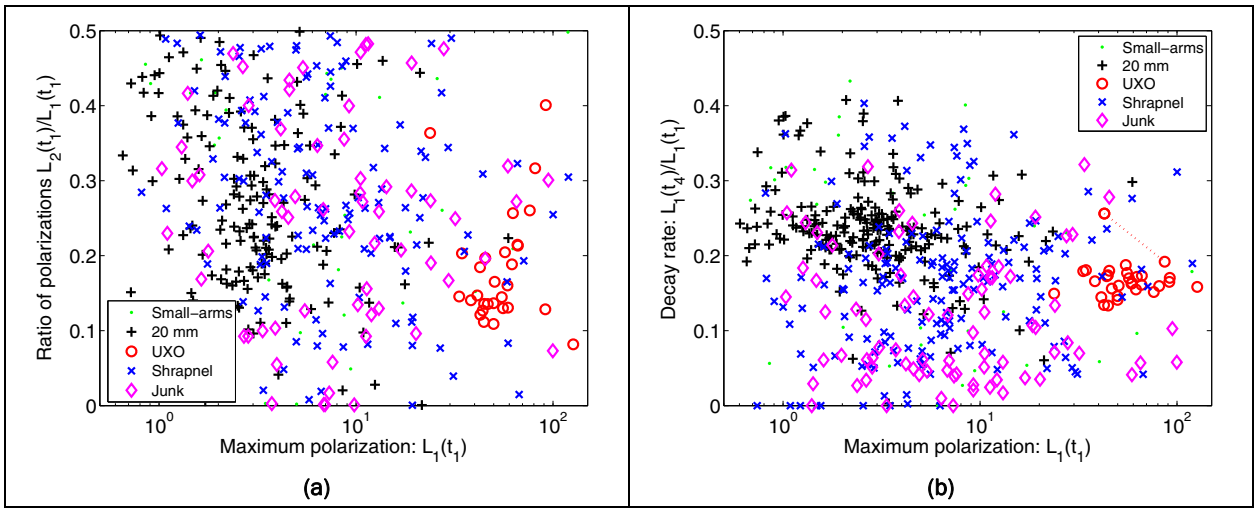

Figure 10. Instantaneous polarization parameters recovered from EM-61 data at all eight rocket range grids. (a) Plot of a shape feature, $L_2(t_1)/L_1(t_1)$ against a size feature, $L_1(t_1)$. (b) Plot of a time-decay feature $L_1(t_4)/L_1(t_1)$ against the same size feature, $L_1(t_1)$. The MK-23 bombs tend to be large and have decay parameters between 0.15 and 0.2.

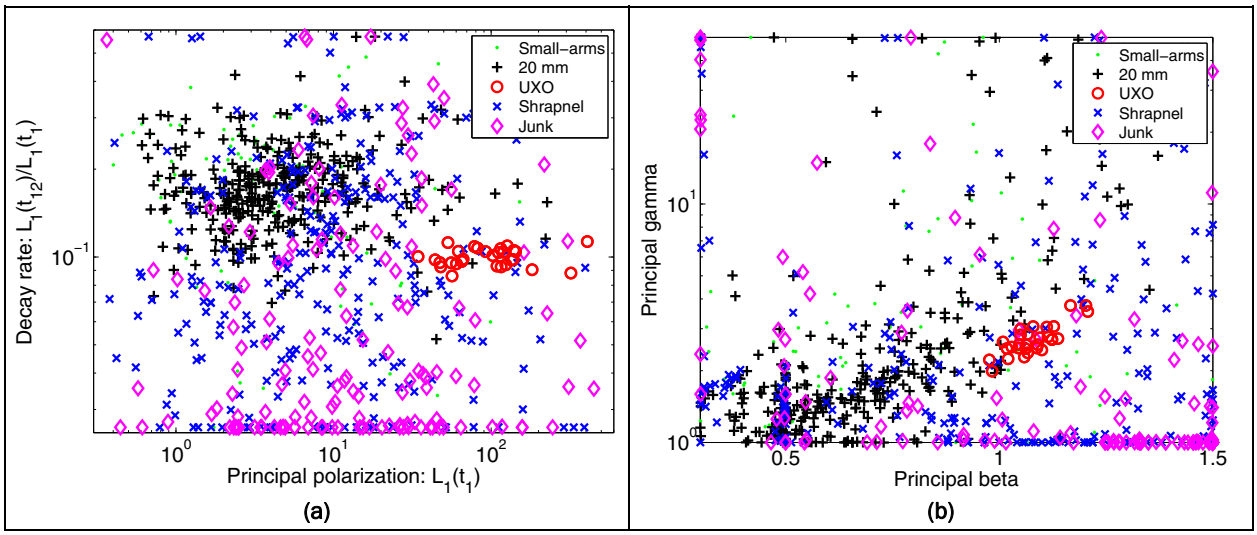

Figure 11. Feature vectors obtained by refitting the EM-63 data at the Rocket Range. (a) Principal polarization, $L_1(t_{12})/L_1(t_1)$ versus $L_1(t_1)$; (b) Transverse polarization, $L_2(t_{12})/L_2(t_1)$ versus $L_2(t_1)$; (c) Principal polarization γ_1 versus β_1.

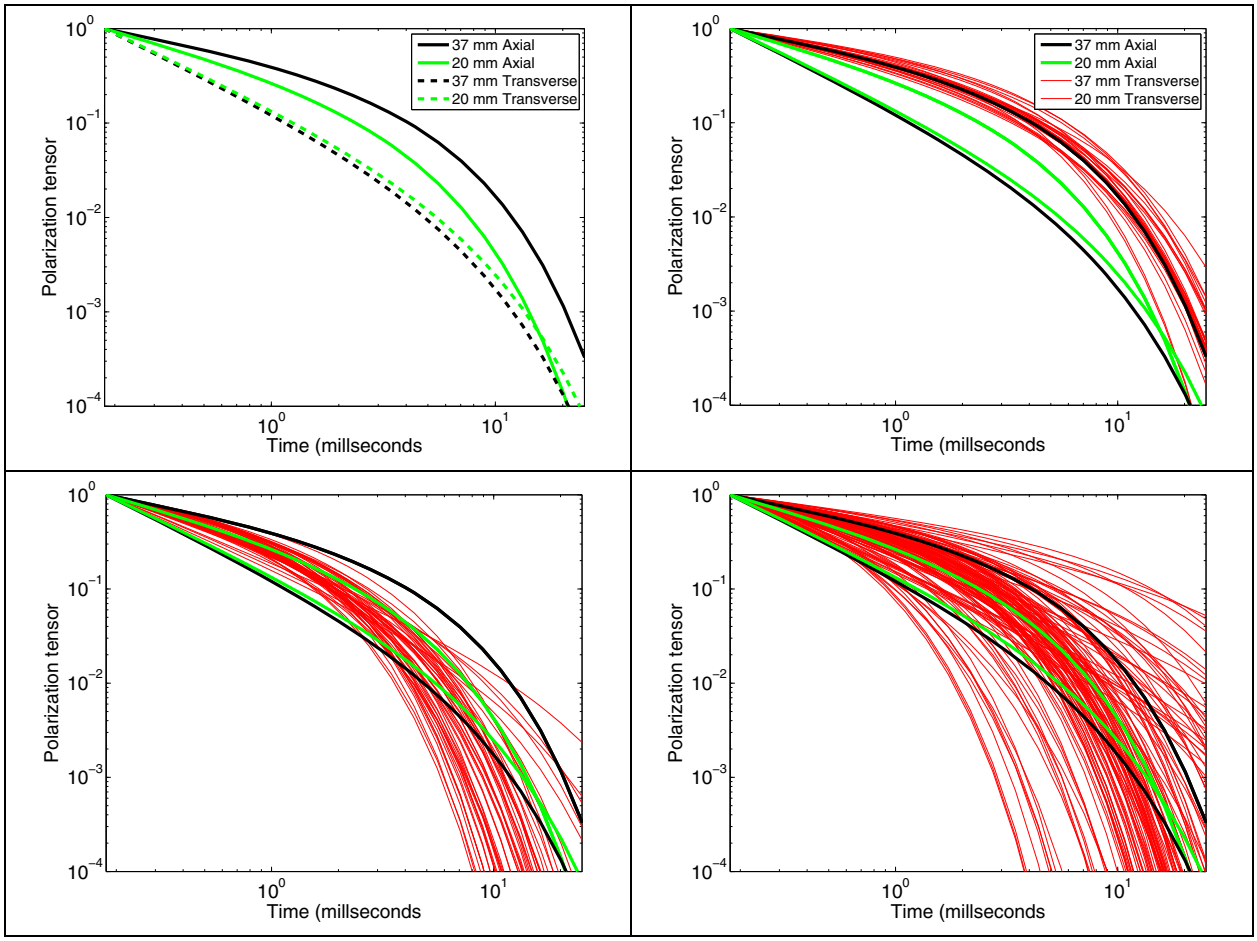

Figure 12. Normalized polarization tensors recovered by inversion for all anomalies on the 20-mm Range Fan. Top left panel: Shows the axial and transverse polarization tensors fit to test stand data over 20- and 37-mm projectiles. Top right panel: Dominant polarizations for 37-mm projectiles. Bottom left panel: Dominant polarization for 20-mm projectiles; Bottom right panel: Dominant polarizations for 50-caliber projectiles.

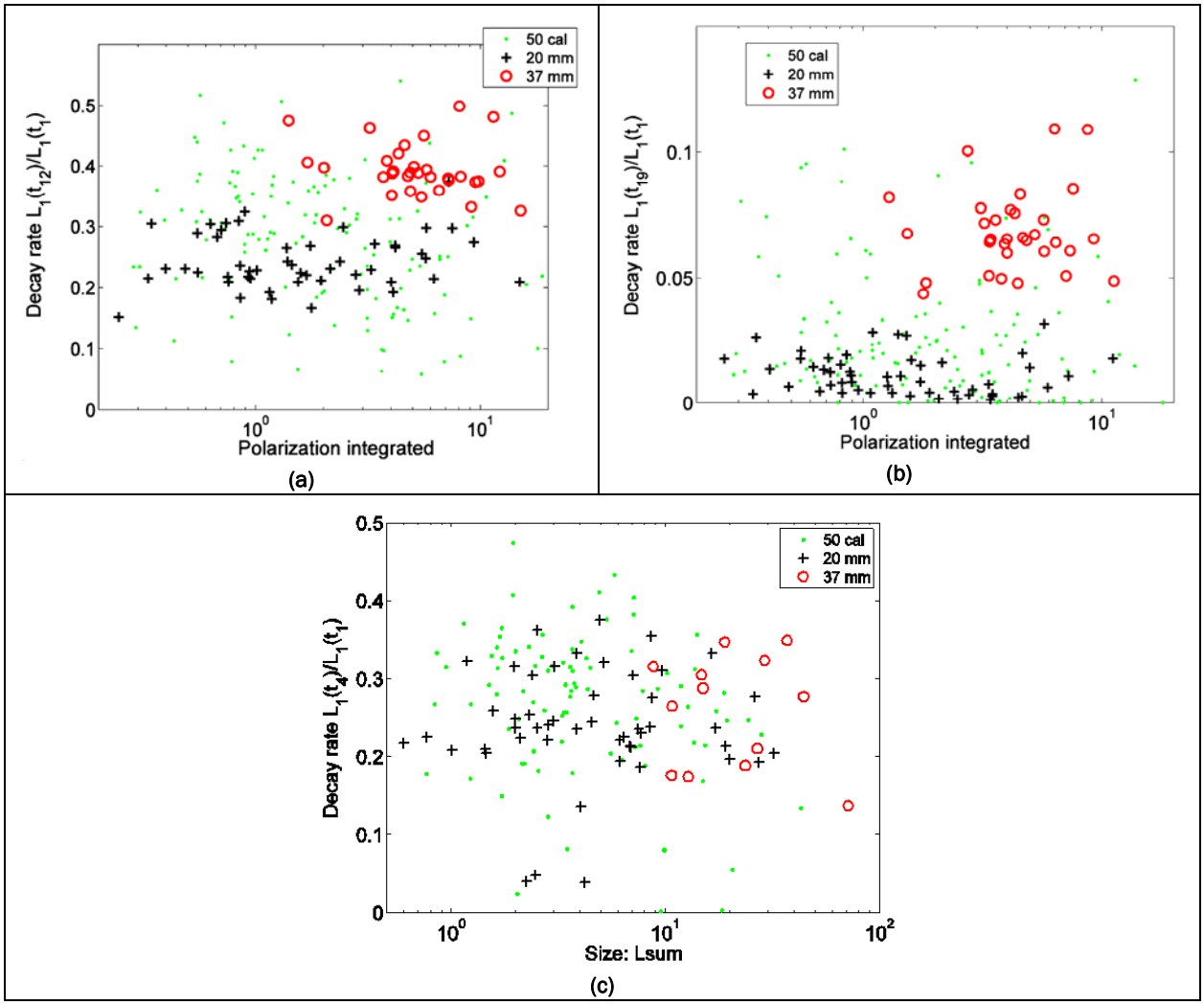

Figure 13. Relative decay rates obtained from the EM-63 (top row) and the EM-61 (bottom row) on the 20-mm Range Fan. The relative decay rates are calculated as the ratio of the principal polarization at time-channels N and 1. (a) EM-63 equivalent to EM-61 with N = 12 (1.1 milliseconds [ms]) over N = 1 (180 microseconds [µs]); (b) EM-63 ratio at N = 19 (5.6 ms) over N = 1; and (c) EM-61 with N = 4 and a ratio of polarizations at 1.2 ms and 216 µs. There is clearly better separation between 37-mm and the other projectiles for the EM-63 at later times.

6.2.2. Comparison of EM-63 data collected in discrimination and cued-interrogation modes

As described in Report 9, cued-interrogation EM-63 data were collected along parallel transects spaced 25 cm apart, with one line collected in an orthogonal direction over the estimated anomaly center. These lanes were pre-marked on a 2.5-m by 2.5-m tarpaulin with data generally collected over a 3-m by 3-m square area centered on the estimated anomaly location. To maximize the signal-to-noise ratio (SNR) and to minimize high-frequency vibrations, the EM-63 suspension cart and RTS/IMU combination used for the discrimination mode data collection were used again.

Three-dipole Pasion-Oldenburg models were fit to the discrimination and cued-interrogation mode datasets.

The higher quality, better positioning and denser coverage of the EM-63 cued-interrogation data (compared to discrimination mode data) result in a significant improvement in the discrimination potential of the system (Figure 14). The primary and secondary polarizations of the 37-mm projectiles and MK-23 practice bombs are more tightly clustered for the cued-interrogation data and agree closely with previously derived test stand values (for the 37-mm projectiles). In addition, the secondary and tertiary polarizations are in close agreement for the 37-mm projectiles and MK-23 practice bombs, so that a feature related to the difference (or spread) in those polarizations has good discrimination potential. This is not the case for the discrimination mode data, where there are often large differences between the secondary and tertiary polarizations. Lastly, both methods return good estimates of the time-decay characteristics of the 37-mm projectiles and MK-23 practice bombs, with significant variations in recovered decays for the smaller 20-mm projectiles (Figure 15).

For the MK-23 practice bombs, using a much richer set of feature vectors from the cued-interrogation mode data could significantly reduce false alarms over the discrimination mode data. For the 37-mm projectiles, a size and a time-decay feature appear to be all that are required for good discrimination performance. Thus, only a marginal improvement in discrimination potential is expected when using cued-interrogation data. Neither method displayed any significant discrimination potential when the target item was a 20-mm projectile.

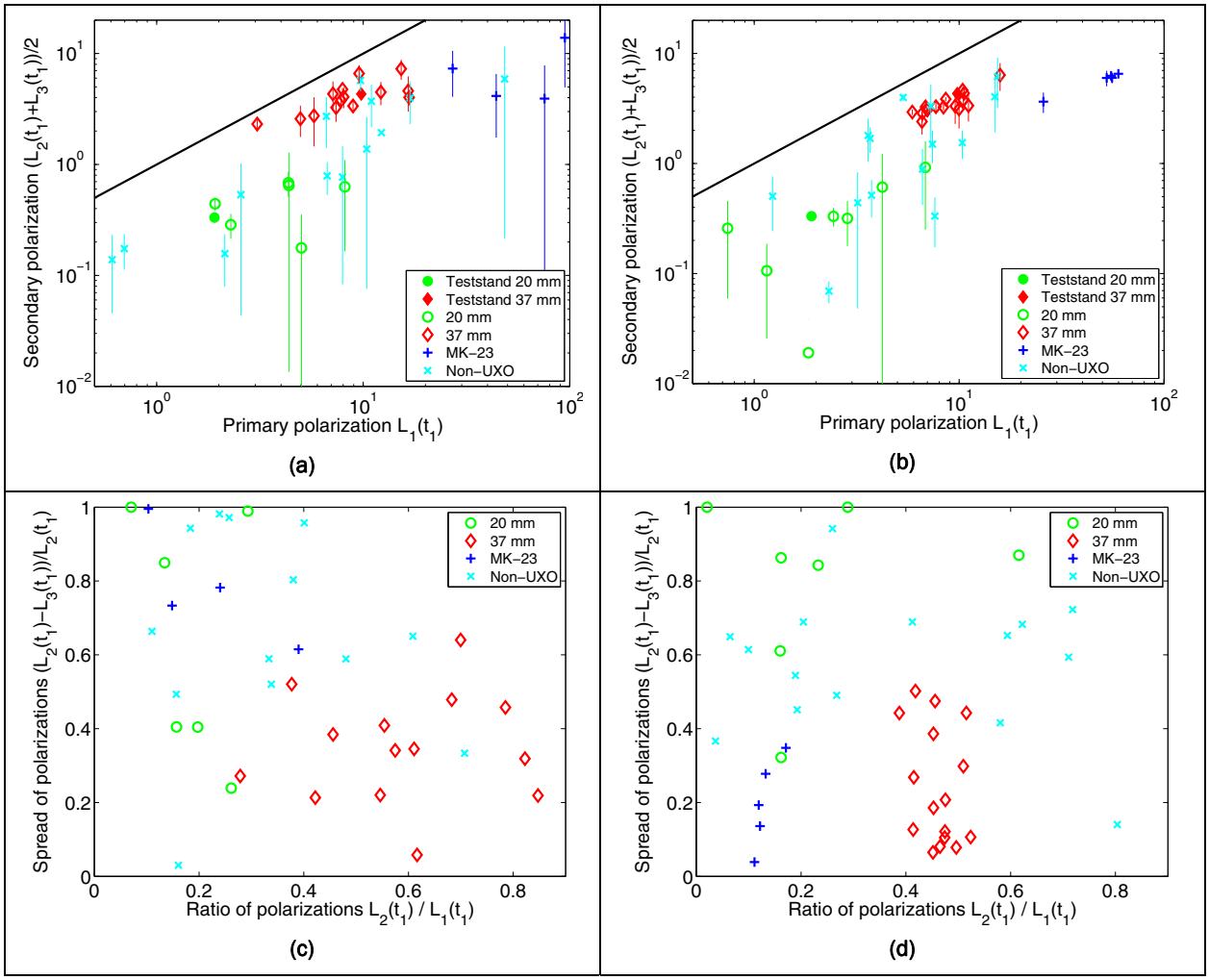

Figure 14. Predicted primary, secondary, and tertiary polarizations of Pasion-Oldenburg models fit to the discrimination (a and c) and cued-interrogation mode (b and d) data. For the secondary polarizations in (a) and (b), the average of the two smaller polarizations are plotted, with a vertical line drawn between the two polarizations. Also shown are the predicted values for the 20- and 37-mm projectiles obtained by inverting test stand data. In (c) and (d) the ratio of secondary to primary polarizations against the spread in the secondary and tertiary polarizations are plotted.

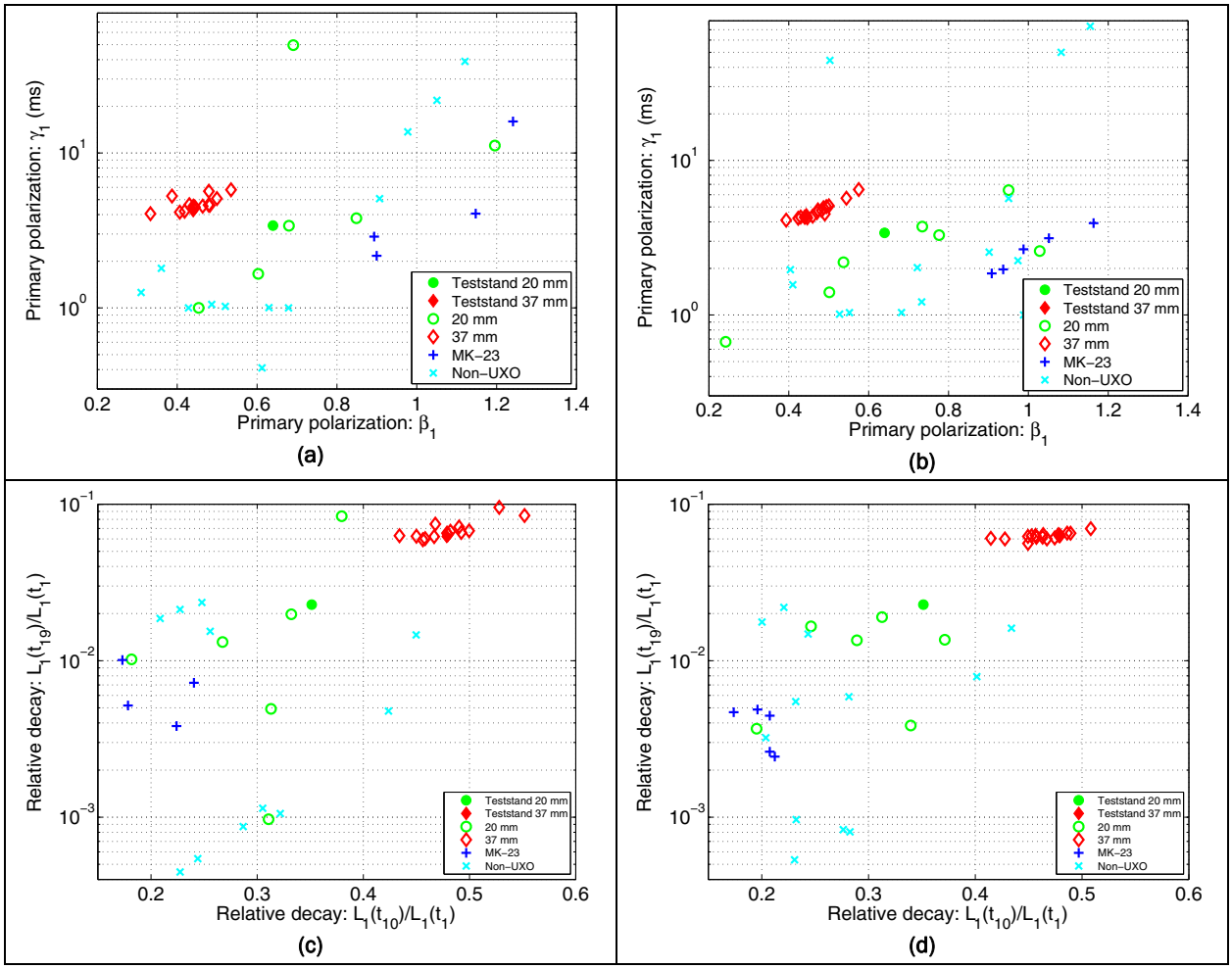

Figure 15. Predicted β and γ parameters for primary polarizations of Pasion-Oldenburg models fit to (a) discrimination and (b) cued-interrogation mode data. Predicted decay rates for the primary polarization of Pasion-Oldenburg models fit to (c) discrimination and (d) cued-interrogation mode data.

6.2.3. Analysis of GEM-3 cued-interrogation mode data

GEM-3 cued-interrogation mode data were collected with the aid of a 1-m by 1-m template consisting of 49 measurement locations. Approximately 5 seconds of data were collected at each location on the template. At the fiftieth survey location, a fiberglass jig was used to collect data at a second elevation (3 cm higher) in the center of the template. Three-dipole instantaneous amplitude models were fit to the GEM-3 data.

The data over 58 GEM-3 anomalies were inverted using a three-dipole instantaneous polarization model (see Report 6). This involved finding the three real and imaginary components of the polarization tensor at each frequency, along with three Euler angles that define the orientation of the item as well as an estimated position and depth.

The instantaneous amplitudes $L(\omega)$ of the three-dipole inversions were fit to the following four-parameter model of Miller et al. (2001)

$$L(\omega) = k\left(s + \frac{(i\omega\tau)^c - 2}{(i\omega\tau)^c + 1}\right) \tag{11}$$

where:

ω = angular frequency
k = object amplitude
s = factor that controls the magnitude of asymptotes at high and low frequency
τ = response time-constant
c = parameter that controls the width of the in-phase peak response (Figure 16).

The parameter plots indicate that the amplitude and time constant provide excellent separation between the hazardous 37-mm projectiles and the nonhazardous 50-caliber bullets and 20-mm projectiles. Some class separation is inherent in the *c*- and *s*-parameter plots, with partial overlap between the 20- and 37-mm parameter spreads.

The amplitude and time-constant features also provide excellent separation between the 50-caliber bullets and the 20-mm projectiles. Within the τ-plot, the two 50-caliber bullets in the 20-mm cluster and the three 20-mm projectiles in the 50-caliber cluster most likely correspond to mislabeled items. All five items were found more than 50 cm from the location estimated from inversion of the GEM-3 data. Given the high density of items found at the site, it's quite likely that an alternate nearby item was mistakenly identified as the anomaly source. The five outliers in the τ-plot are the same five outliers in the amplitude plot (the three lowest amplitude 20-mm projectiles and the two high-amplitude 50-caliber bullets).

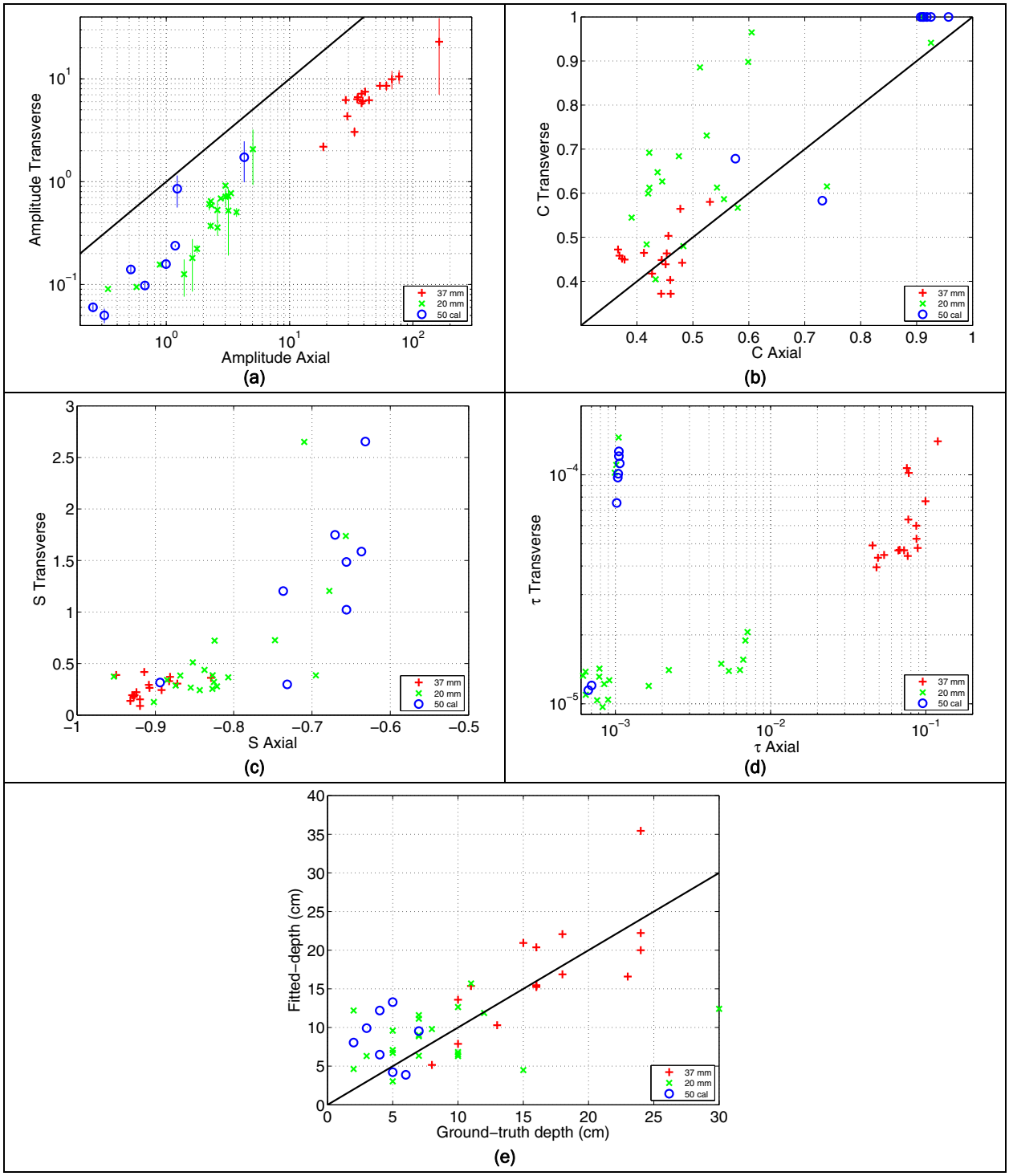

Figure 16. Polarization tensor parameter recovered from GEM-3 data collected at the 20-mm Range Fan: (a) Amplitude of the Miller et al. (2001) model; (b) Miller *c* parameter; (c) Miller *s* parameter; (d) Miller time-constant parameter; and (e) actual versus predicted depth.

6.2.4. Summary

For the EM-63, the following features provide useful discrimination information for both the 37-mm projectiles and MK-23 practice bombs.

- The size of the primary polarization (either $L_1(t_1)$ or the integrated polarization);
- The time decay (must be very fast for an MK-23);
- For the cued-interrogation mode data only, the difference between the secondary and tertiary polarizations.
- For the cued-interrogation mode data only, the ratio of the secondary to primary polarizations;

In summary,

- For the MK-23 practice bombs, a much richer set of feature vectors from the cued-interrogation mode data could be used, which could potentially significantly reduce false alarms over the discrimination mode data;
- For 37-mm projectiles, a size and a time-decay feature appear to be all that are required for good discrimination performance on 37-mm projectiles. Thus, only a marginal improvement in discrimination potential is expected when using cued-interrogation data.
- Neither method displayed any significant discrimination potential if the munition of concern was a 20-mm projectile.

Additional details on the discrimination and cued-interrogation mode data can be found in Billings et al. (2007) and Report 9.

For the GEM-3 data, which were collected in cued-interrogation mode, the amplitude and time constants of the four-parameter model of Miller et al. (2001) appeared to provide good discrimination potential. In particular:

- All 37-mm projectiles could be clearly distinguished from 50-caliber bullets and 20-mm projectiles;
- Except for five items (suspect to be mislabeled), the 50-caliber bullets and 20-mm projectiles were well separated in feature space.

Thus, when deployed in a cued-interrogation mode, the GEM-3 appears to be capable of distinguishing 37-mm projectiles from 20-mm projectiles AND of distinguishing 20-mm projectiles from 50-caliber bullets. While

this result is extremely promising, it should be kept in mind that the data collection process required a template and was relatively slow. To provide a practical solution to this small object discrimination problem, much faster data collection rates need to be achieved.

7 Summary and Conclusions

The research conducted under this project focused on determining the unexploded ordnance (UXO) discrimination potential of various sensor phenomenologies, deployment modes, and processing strategies. Sensor phenomenologies explored included ground penetrating radar (GPR), total-field magnetics, and time- and frequency-domain electromagnetic induction (TEM and FEM). Deployment modes developed included towed-array, cart-based, and man-portable in both discrimination and cued-interrogation modes. Processing strategies considered included static-dipole (for magnetics), polarization tensor, and physically complete approaches for electromagnetic induction.

Even at a "favorable" site, UXO detection performance with a GPR system will vary throughout the year and will be dependant on the past weather conditions at the site. A multi-frequency, multi-polarimetric system was found to have the most promise and would be suitable for deployment as a confirmation sensor, particularly when the GPR interpretation is constrained by magnetic or electromagnetic data.

The first live site visited in this project was the Marine Corps Base Camp Lejeune in North Carolina. Ubiquitous aluminum adapters present on site created a significant and unique discrimination challenge. A large number of aluminum 40-mm grenades were also found at the site. The insensitivity of magnetometry to non-ferrous metals made it an ideal technique for rejecting false alarms due to the ubiquitous adapters present on the site. However, this same argument precluded using the technique for detection of the 40-mm grenades. For the EM-61 towed array, the relative size of primary and secondary polarizations allowed many adapters to be rejected. The relative decay rate of the primary or secondary polarizations was effective in distinguishing many of the remaining adapters from the UXO. The standard deviation in a 0.5 m radius of the corresponding magnetic data was also highly discriminatory against the adapters. For the EM-63 cart data, the decay of the secondary polarization of the adapters was significantly different than that of any of the UXO. The longer measurement time of the EM-63 resulted in superior discrimination performance to the EM-61 and obviated the need for supplemental magnetic data. For the UXO/adapter discrimination problem, the EM-61/magnetometer

combination had performance comparable to the EM-63 alone. When the 40-mm grenades were included as potential UXO, the EM-63 significantly outperformed the EM-61/magnetometer combination.

The second live site visited was the Former Lowry Bombing and Gunnery Range in Colorado. Two ranges were surveyed. The objectives of the Rocket Range surveys were the discrimination of a mixed range of projectiles with minimum diameter of 37 mm from shrapnel, junk, 20-mm projectiles, and small arms. The main ordnance item encountered was an MK-23 practice bomb. The 20-mm Range Fan survey presented a small-item discrimination scenario, where the objective was to discriminate 37-mm projectiles from ubiquitous 20-mm projectiles and 50-caliber bullets.

The higher quality, better positioning, and denser coverage of the EM-63 cued-interrogation data (compared to discrimination mode data) result in a significant improvement in the discrimination potential of the system. For the MK-23 practice bombs, using a much richer set of feature vectors from the cued-interrogation mode data could potentially significantly reduce false alarms over the discrimination mode data. For the 37-mm projectiles, a size and a time-decay feature appear to be all that are required for good discrimination performance. The EM-63 did not display any significant discrimination potential when the target item was a 20-mm projectile.

For the GEM-3 data, all 37-mm projectiles could be clearly distinguished from 50-caliber bullets and 20-mm projectiles. The 50-caliber bullets and 20-mm projectiles were well separated in feature space. Thus, when deployed in a cued-interrogation mode, the GEM-3 appears to be capable of distinguishing 37-mm projectiles from 20-mm projectiles AND of distinguishing 20-mm projectiles from 50-caliber bullets.

One of the primary objectives of this project was to determine if the extra cost and effort involved in collecting and processing cued-interrogation data would be recouped through savings in the number of items excavated. At the Ashland test plot and the FLBGR live site feature vectors extracted from cued-interrogation data were demonstrated to be more accurate and reliable than those extracted from discrimination mode data. In addition, a much richer set of feature vectors could be used to aid UXO discrimination. Those additional feature vectors were not always required: for

example, at the 20-mm Range Fan, hazardous 37-mm projectiles could be distinguished from 20-mm projectiles and 50-caliber bullets using size and time-decay features extracted from discrimination mode data.

The most cost-effective deployment mode (cued or discrimination) will depend on the particular discrimination scenario (i.e., what type of ordnance and clutter occur on the site, the geological background, etc.) and on the cost of excavation of each suspected ordnance item. Where the costs of excavating items is high (e.g., chemical filled rounds, excavation near populated areas), cued interrogation is likely to be more cost-effective than collection of discrimination mode data because even small improvements in discrimination performance will reduce costs considerably. In contrast, where excavation costs are low (e.g., excavation of shallow, small items), discrimination mode data collection will be more cost-effective, as the extra costs of collecting the cued data won't be recouped through reduced excavation costs. In conclusion, the author feels that cued interrogation has a role to play in UXO clearance, but that it is a tool that should only be applied when the discrimination challenge is too difficult to be solved by discrimination mode data collection.

In conclusion, COTS magnetometer and electromagnetic induction sensors were used for successful discrimination at each of the test and live sites visited. In each case, accurate position and orientation information and careful data collection, processing, and inversion were required to allow accurate feature vectors to be extracted over each detected anomaly. Once extracted, and with appropriate training data, effective discrimination strategies could be developed with the aid of statistical classification algorithms. Each site presented a different and novel discrimination challenge. This means that multiple sensors, deployment modes, and interpretation strategies are required to tackle the diversity of UXO-contaminated sites in the continental United States, and elsewhere.

References

Billings, S. D., L. R. Pasion, L. Beran, D. W. Oldenburg, D. Sinex, L. Song, and N. Lhomme. 2007. Demonstration Report for the Former Lowry Bombing and Gunnery Range, ESTCP MM-0504: Practical Discrimination Strategies for Application to Live Sites.

Miller, J. T., T. H. Bell, J. Soukup, and D. Keiswetter. 2001. Simple phenomenological models for wide-band frequency domain electromagnetic induction. In *IEEE Transactions on Geoscience and Remote Sensing* 39:1294–1298.

Pasion, L. P., N. Lhomme, L. P. Song, F. Shubitidze, and D. W. Oldenburg. 2006. *A unified approach to UXO discrimination using the Method of Auxiliary Sources*. SERDP-UX-1446 Final Report.

Pasion, L. P., S. D. Billings, D. W. Oldenburg, and S. E. Walker. 2007. Application of a library-based method to time domain electromagnetic data for the identification of unexploded ordnance. *Journal of Applied Geophysics* 61:279–291.

Shubitidze, F., K. ONeill, I. Shamatava, K. Sun, and K. D. Paulsen. 2005a. A simple magnetic charge model for classification of multiple buried metallic objects in cases with overlapping signals. In *Proceedings*, *SAGEEP 05*.

_____. 2005b. Fast and accurate calculation of physically complete EMI response by a heterogeneous metallic object. In *IEEE Transactions of Geoscience and Remote Sensing* 43:1736–1750.

REPORT DOCUMENTATION PAGE

Form Approved
OMB No. 0704-0188

1. REPORT DATE *(DD-MM-YYYY)*	2. REPORT TYPE	3. DATES COVERED *(From - To)*
September 2008	Report 1 of 9	

4. TITLE AND SUBTITLE

UXO Characterization: Comparing Cued Surveying to Standard Detection and Discrimination Approaches: Report 1 of 9 – Summary Report

5a. CONTRACT NUMBER
W912HZ-04-C-0039

5b. GRANT NUMBER

5c. PROGRAM ELEMENT NUMBER

6. AUTHOR(S)

Stephen D. Billings

5d. PROJECT NUMBER

5e. TASK NUMBER

5f. WORK UNIT NUMBER

7. PERFORMING ORGANIZATION NAME(S) AND ADDRESS(ES)

Sky Research, Inc.
445 Dead Indian Memorial Road
Ashland, OR 97520

8. PERFORMING ORGANIZATION REPORT NUMBER

ERDC/EL TR-08-32

9. SPONSORING / MONITORING AGENCY NAME(S) AND ADDRESS(ES)

Headquarters, U.S. Army Corps of Engineers
Washington, DC 20314-1000;
U.S. Army Engineer Research and Development Center
Environmental Laboratory
3909 Halls Ferry Road, Vicksburg, MS 39180-6199

10. SPONSOR/MONITOR'S ACRONYM(S)

11. SPONSOR/MONITOR'S REPORT NUMBER(S)

12. DISTRIBUTION / AVAILABILITY STATEMENT

Approved for public release; distribution is unlimited.

13. SUPPLEMENTARY NOTES

14. ABSTRACT

This report summarizes research conducted under W912HZ-04-C-0039 and highlights the most important results obtained. This project focused on determining the UXO discrimination potential of various sensor phenomenologies (ground penetrating radar, total-field magnetics, and time- and frequency-domain EMI), deployment modes, and processing strategies. Magnetometer and EMI sensors could be used for successful discrimination at each of the study sites. In each case, accurate position and orientation information and careful data collection, processing, and inversion were required to allow accurate feature vectors to be extracted over each detected anomaly. Once extracted, and with appropriate training data, effective discrimination strategies could be developed with the aid of statistical classification algorithms. Each site presented a different and novel discrimination challenge; multiple sensors, deployment modes, and interpretation strategies are required to tackle the diversity of UXO-contaminated sites in the United States and elsewhere.

15. SUBJECT TERMS

EMI sensors
Ground penetrating radar
Total-field magnetics
Frequency-domain electromagnetic induction (FEM)
Time-domain electromagnetic induction (TEM)
Unexploded ordnance (UXO)
UXO discrimination

16. SECURITY CLASSIFICATION OF:			17. LIMITATION OF ABSTRACT	18. NUMBER OF PAGES	19a. NAME OF RESPONSIBLE PERSON
a. REPORT	b. ABSTRACT	c. THIS PAGE			19b. TELEPHONE NUMBER *(include area code)*
UNCLASSIFIED	UNCLASSIFIED	UNCLASSIFIED		52	